Environmental Impact Assessment Review 118 (2026) 108297

Contents lists available at ScienceDirect

Environmental Impact Assessment Review

journal homepage: www.elsevier.com/locate/eiar

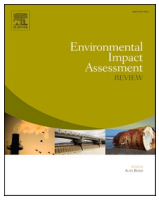

Multivariate environmental and social life cycle assessment of circular recycled-plastic voided slabs for data-driven sustainable construction

Antonio J. Sánchez-Garrido [a,*,1], Ignacio J. Navarro [a,2], Víctor Yepes [b,2]

[a] Dept. of Construction Engineering, Universitat Politècnica de València, Valencia 46022, Spain
[b] Institute of Concrete Science and Technology (ICITECH), Universitat Politècnica de València, Valencia 46022, Spain

ARTICLE INFO

Keywords:
Circular economy
Life cycle assessment
Sustainable construction
Low-carbon building design
Voided biaxial slabs
Embodied carbon
Multivariate analysis

ABSTRACT

The construction sector is a major contributor to climate change and resource depletion, responsible for over 36 % of global final energy use and nearly half of all raw material consumption. Addressing structural systems' environmental and social sustainability is a critical challenge for the transition toward a circular and low-carbon built environment. Among structural elements, floor slabs are particularly critical due to their intensive use of concrete and steel. This study develops an integrated, data-driven framework that combines multivariate structural modeling with environmental and social life cycle assessment (*E*-LCA and S-LCA), explicitly describing the methodological approach before results are introduced. Leveraging empirical data from 67 real buildings, the framework generates robust pre-dimensioning guidelines that support early-stage decision-making in sustainable construction. Results demonstrate substantial material and impact reductions: concrete and steel use decrease by 23–33 % and up to 29 %, respectively, leading to average endpoint environmental impact reductions of 25 % and global warming potential decreases of 24 %, reaching 30 % for six-meter spans. S-LCA highlights social risk reductions up to 20 % in the Workers and Local Community categories, reflecting safer and more socially responsible construction practices. By integrating advanced multivariate modeling with comprehensive life cycle assessment, this research delivers a decision-oriented tool that accelerates the adoption of circular, low-carbon construction systems. The revised abstract also highlights the policy and management implications: the findings provide actionable insights for engineers, regulators, and policymakers, supporting the development of building codes, resource-efficient design guidelines, and climate-aligned strategies for the construction sector. Ultimately, this work promotes a resilient and sustainable built environment, advancing circular economy principles and the United Nations Sustainable Development Goals (SDGs).

1. Introduction

Accelerated urbanization has positioned construction as a central driver of global economic activity and employment. Over the past 70 years, the world's urban population has increased from 30 % to 56 % (Scrucca et al., 2023). The built environment requires vast amounts of raw materials and energy, with construction accounting for approximately 50 % of material use and 36 % of total energy consumption worldwide (Norouzi et al., 2021). Climate mitigation and cleaner production strategies are therefore imperative in this sector. By 2050, emissions from new construction could account for 50 % of global CO_2 output—up from 28 % today—while total material demand may exceed 90 billion tons (MacArthur and Heading, 2019). Rising material costs are prompting the industry to adopt reuse, recycling, and resource optimization strategies (Metinal and Gumusburun Ayalp, 2025). Aligning construction practices with the Sustainable Development Goals (SDGs) is now a global priority, integrating economic growth, social equity, and environmental protection under the Circular Economy (CE) framework, which promotes resource efficiency and waste reduction (Ding et al., 2025; Barbhuiya et al., 2024).

Within the built environment, CE implementation focuses on two core dimensions: material circularity—how efficiently resource loops are reduced, slowed, or closed—and sustainability, encompassing environmental, economic, and social performance (Josa and Borrion,

* Corresponding author.
E-mail addresses: ajsangar@doctor.upv.es (A.J. Sánchez-Garrido), ignamar1@cam.upv.es (I.J. Navarro), vyepesp@cst.upv.es (V. Yepes).
[1] First Author.
[2] Co-Authors.

https://doi.org/10.1016/j.eiar.2025.108297
Received 13 August 2025; Received in revised form 10 November 2025; Accepted 1 December 2025
Available online 5 December 2025

2025). Buildings and infrastructure enhance circularity by minimizing waste and reducing the use of primary materials, allowing for disassembly and reuse, extending service life through maintenance, incorporating recycled materials, and recovering value from waste streams (Li et al., 2022). However, the adoption of CE principles remains limited due to the lack of standardized, integrative assessment frameworks that address all sustainability pillars. The social dimension, in particular, is often overlooked (Navarro et al., 2024). Life Cycle Assessment (LCA), Social Life Cycle Assessment (S-LCA), and Life Cycle Cost Assessment (LCCA) are key tools for quantifying performance across these three dimensions; however, data availability continues to constrain comprehensive applications (Patrisia et al., 2025). Recent methodological progress—such as the organizational S-LCA developments by Traverso and Mankaa (2025)—points toward greater integration, but practical implementation in construction remains fragmentary. Consequently, many studies emphasize environmental impacts while cost and social implications are only partially considered. Moreover, the inclusion of Life Cycle Cost Assessment remains limited by the scarcity of reliable economic datasets, highlighting the need for future research that systematically integrates LCCA alongside environmental and social indicators.

Among structural components, floor slabs exhibit the highest environmental impact due to their extensive material volume (Feiri et al., 2024). Cement production alone accounts for 5–7 % of global CO_2 emissions, making the cement industry a key target for emission reduction. Shanks et al. (2019) showed that improving material efficiency through design optimization could halve emissions, highlighting slabs as a strategic priority. Conventional reinforced concrete slabs—one-way or two-way—require increased thickness for long spans, resulting in higher concrete volumes and heavier loads, which in turn enlarge beams, columns, and foundations (Poudel and Gyawali, 2025). To address these inefficiencies, Modern Methods of Construction (MMC) are being deployed to enhance productivity, safety, and sustainability (Sánchez-Garrido et al., 2022; Hernández et al., 2023; Hafez et al., 2024). The convergence of AI-based design tools, Building Information Modeling (BIM), and life-cycle thinking is accelerating this shift toward digital, data-driven construction (Campo Gay et al., 2024). These advances align with ongoing efforts to develop optimized safety frameworks and sustainable design methodologies for structural systems (Sánchez-Garrido et al., 2026).

Innovation in slab systems focuses on material reduction by eliminating non-structural concrete zones. Plastic void formers placed between reinforcement layers reduce self-weight without compromising performance (Pawar et al., 2024a). Biaxial voided slabs (VS) replace concrete with spherical, cubic, or disc-shaped voids, reducing dead weight by up to 35 % compared with conventional solid slabs (CS) (Chung et al., 2022), and even up to 50 % when optimized (Pawar et al., 2024b). Advantages include lower seismic loads, longer spans, reduced structural height, faster assembly, and inherent fire resistance (Fanella et al., 2017; Sánchez-Garrido et al., 2024). Despite these benefits, research on environmental and circular performance remains limited, with a focus primarily on CO_2 emissions during production and construction (Paik and Na, 2019a; Paik et al., 2019). Sustainability-oriented studies have also highlighted the potential of incorporating recycled waste plastics as void formers (Ferdous et al., 2021), reinforcing the circularity rationale for using secondary materials in such systems. Previous analytical and experimental studies have thoroughly characterized the structural performance of voided slabs. Chung et al. (2018a, 2018b) analyzed the flexural and punching-shear behavior of two-way slabs with doughnut-shaped voids, while Al-Gasham et al. (2019) and Valivonis et al. (2017) showed that voids near slab–column connections reduce shear capacity, requiring solid zones for mitigation. Amoushahi Khouzani et al. (2020) quantified the influence of ellipsoidal void shapes and distribution on shear strength. In contrast, Sagadevan and Rao (2019) and Subramanian et al. (2017) evaluated how spherical versus cubic voids and increased spacing improve stiffness and load–deflection response. These findings provide key design guidance and demonstrate both the opportunities and challenges of optimizing material efficiency without compromising structural integrity.

Recent studies based on LCA highlight similar methodological gaps. Pavlů et al. (2023) analyzed recycled-aggregate concrete slabs under different limit states, demonstrating environmental benefits but without linking them to spatial or social indicators. Tsui et al. (2024) provided spatial criteria for circular construction hubs, emphasizing urban form as a determinant of material efficiency. Lotz et al. (2024) mapped the service-stock-flow dynamics of steel and concrete in European buildings, showing national disparities that influence embodied impacts. Guaygua et al. (2024) conducted an LCA of modular prefabricated buildings with seismic resilience, while Shen et al. (2024) developed high-resolution mapping of residential building stock to quantify material intensity. Collectively, these studies underscore the increasing convergence of spatial and environmental analysis in the built environment, yet few explicitly couple Life Cycle Assessment with structural system modeling or circularity metrics at the component level. In the context of data-driven design, multivariate and regression-based approaches offer quantitative insights for optimizing slab configurations and identifying key variables that influence performance. Previous works have employed structured databases and multivariate models for pre-dimensioning and ANOVA-based variable significance testing (Paranhos and Petter, 2013), while Lase et al. (2021) demonstrated their capacity to address collinearity and interdependence among design parameters. Such approaches align with the present study's aim to combine empirical evidence and statistical modeling to derive predictive sustainability indicators.

Amid growing demand for circular, low-carbon structures, this study addresses a critical knowledge gap by combining multivariate statistical modeling with environmental and social life-cycle analysis (LCA and S-LCA) of voided slab systems. The research focuses on a novel two-way flat reinforced concrete slab without beams, which is lightened with recycled plastic spheres or discs and is fully recyclable after service (Yang et al., 2025). Despite clear advantages, the technology remains underrepresented in standardized codes. Building upon recent advances in circularity assessment (Li et al., 2022; Barbhuiya et al., 2024) and organizational S-LCA (Traverso and Mankaa, 2025), this work quantifies material efficiency, embodied impacts, and social performance across 67 real buildings. It also stratifies results by spatial typology (rural/sub-urban, urban, and high-density urban) to link material demand with land-use intensity, bridging micro-scale structural optimization and macro-scale planning relevance. By deriving predictive design models and sustainability metrics from empirical data, this study provides practical decision-support tools for engineers and planners seeking to accelerate circular, data-driven construction transitions.

2. Materials and methods

The analyzed construction system consists of an innovative flat, two-way reinforced concrete biaxial voided slab (VS) without beams, lightened by pressurized recycled plastic void formers—spheres or discs made from 100 % recycled plastic, designed for reintegration into production at end-of-life, enhancing sustainability. As shown in Fig. 1, discs suit slabs 15–28 cm thick, spheres for 28–42 cm. Lacking official standards or design codes, statistical analysis developed pre-dimensioning rules based on minimal variables, producing a streamlined predictive model applied to slabs with 6 m and 12 m column spans. A solid zone around columns for punching shear resistance was defined with a radius of one-sixth the span. Concrete compressive strength was 25 MPa, and the live load was 2 kN/m^2. Environmental and social life cycle assessments (LCA and S-LCA) employed a cradle-to-grave approach, comparing impacts against a conventional slab (CS), defined for simplicity as a bidirectional ribbed/waffle reinforced concrete slab with expanded polystyrene (EPS) blocks, supported on beams. CS slabs have ribs visible on the soffit, since only a thin compression layer covers the

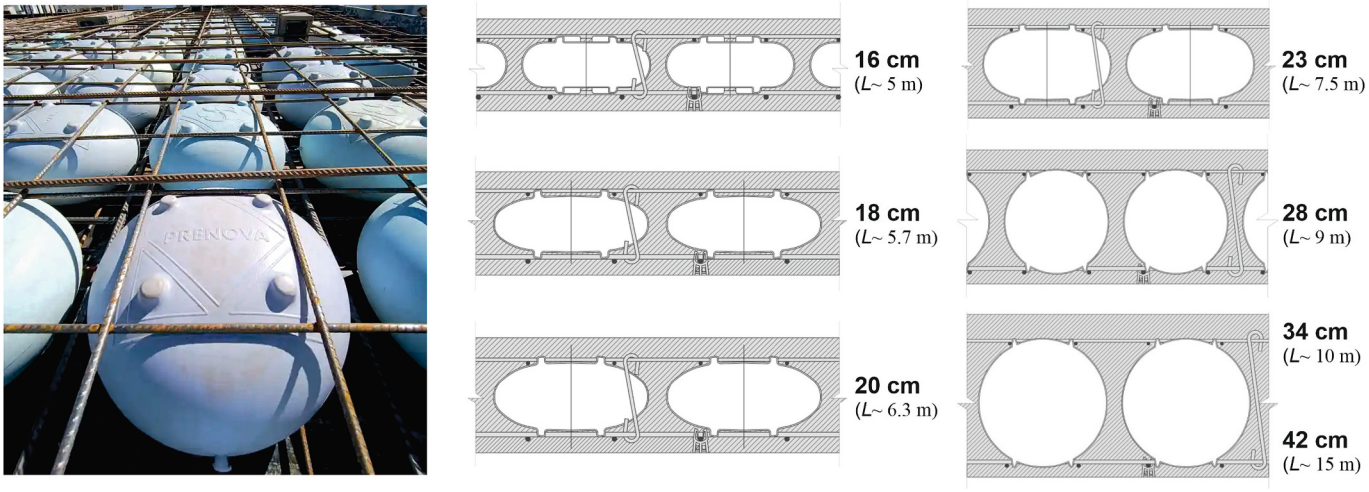

Fig. 1. Lightweight PRENOVA slab using plastic void formers at varying thicknesses.

top, while EPS blocks shape the ribs and remain exposed underneath. In contrast, voided slabs (VS) have continuous top and bottom layers of concrete, with recycled plastic voids embedded in the core, so the soffit remains flat like a solid slab.

2.1. Multivariate analysis

Multivariate analysis is essential for datasets with correlated variables. This study analyzed 75 slab observations from 67 real buildings using VS lightening systems, with spans ranging from 5.2 to 15 m and slab thicknesses between 16 and 42 cm. Appendix B provides details: sampling framework (Table B.1), typologies (Table B.2), and data matrices for the initial, adjusted, and final Statgraphics models (Tables B.3–B.5), corresponding to Eqs. 1–3. To enhance the interpretability of the dataset for planning-oriented applications, each case study in Table B.2 was classified according to spatial typology, integrating vertical (number of floors) and horizontal (slab area) indicators. Three categories were defined: Rural/Suburban ($\leq$2 floors and $<$ 1000 m^2), Urban (3–7 floors or 1000–5000 m^2), and High-Density Urban ($\geq$8 floors or $>$ 5000 m^2). This combined criterion provides a proxy for built density and land-use intensity, ensuring that low-rise but large-footprint buildings such as airports or industrial complexes are properly captured as high-density contexts. The classification enables linking building scale and density with the environmental and social life-cycle outcomes analyzed in subsequent sections.

The analysis followed three stages: exploratory data analysis to assess distributions and relationships, two-variable modeling to identify initial correlations, and multivariate modeling to refine predictions considering interactions. Table 1 summarizes key parameters: central span, thickness, void former type and size (disc height or sphere diameter), estimated live loads, construction year, and floor count. Descriptive statistics—mean, coefficient of variation, and percentiles (25th, 50th, 75th)—provide an overview of variability. The first six variables show close means and medians, indicating slight distribution asymmetry.

The primary relationship between the main span (L) and the thickness of the lightened slab (t) was analyzed as a preliminary step. An initial model approximation was developed using simple linear regression, fitting a line to the scatter plot through the least squares method with a 95 % confidence level. t was treated as the dependent variable, and L was the independent variable. Outlier residuals were analyzed to ensure data consistency. This first model will select the height of the plastic disc or sphere based on commercially available sizes.

The second model was refined through multivariate regression analysis by incorporating additional variables: height of the disc or sphere (H_e), most probable live load (Q_1), alternative live load (Q_2), and span squared (L^2). Correlation and covariance statistics were used to identify which independent variables had a strong relationship with t. Studentized residuals helped detect outliers, defined as observations more than two standard deviations from the fitted model, which were examined and treated to improve data quality.

Finally, a third and more refined model was obtained by multiple regression using the significant variables selected from the previous step. The least squares fitted this model to explain the response variable to the greatest extent possible. The goodness of fit was assessed by the coefficient of determination (R^2), representing the proportion of variation explained by the model. Additionally, the Durbin-Watson statistic was applied to check for autocorrelation in residuals, and outlier residuals were analyzed to confirm the model's robustness.

Table 1
Descriptive statistics of geometric, load, and temporal parameters for lightweight biaxial slabs (n = 75).

Parameter	Average	C.V. (%)	Min.	Max.	P25/Q1	P50/Q2/Med	P75/Q3
Main span (m)	7.64	24.19	5.20	15.00	6.15	7.20	9.00
Slab thickness (cm)	23.99	25.00	16	42	20.00	23.00	28.00
Disc or sphere height (cm)	15.02	20.02	10.00	18.00	12.00	14.00	18.00
Diameter of the sphere (cm)	24.29	10.98	21.00	27.00	22.00	22.00	27.00
Primary live load (kN/m^2)	2.69	41.49	2.00	5.00	2.00	2.00	3.00
Secondary live load (kN/m^2)	2.70	40.29	1.00	4.00	1.50	3.00	3.00
Slab surface (m^2)	4938.37	153.93	160.00	45,000.00	742.50	1750.00	5900.00
End of construction (year)	2012	0.13	2006	2018	2011	2012	2013
Number of floors	5.73	80.84	1	26	3	4	7

2.2. Environmental and social life cycle assessment (LCA and S-LCA)

Environmental and social assessments were based on a standardized four-stage methodology: (i) goal and scope definition, including the functional unit and life cycle stages; (ii) inventory analysis of inputs and outputs within system boundaries; (iii) impact assessment, detailing methods for environmental and social evaluation; and (iv) interpretation of results. This structure ensured a robust and systematic evaluation.

A key methodological challenge in incorporating recycled plastic spheres or discs in the slab system is allocating environmental burdens from secondary materials. Following ISO 14044 and the conventions of Ecoinvent v3.2, this study applied the widely accepted cut-off allocation method (Gravina et al., 2021; Visintin et al., 2020). In this approach, products from primary raw materials bear the complete extraction and processing burdens, while secondary materials inherit only the burdens associated with their recycling process. Accordingly, recycled plastic in the VS system was assigned impacts solely from recycling, thereby avoiding the artificial attribution of virgin plastic production impacts and ensuring consistency across environmental and social assessments. In line with ISO 14044, a 1 % cut-off criterion was applied, ensuring that inventory flows with negligible influence on comparative results were excluded from the system boundaries. Minor construction materials such as plasterboard, glass, aluminum, paints, insulation, or copper were therefore modeled using Ecoinvent datasets but not explicitly reported, since their contribution to total impacts remained below the threshold.

The assessment's first stage aimed to evaluate the VS life cycle performance using a functional unit of 1 m^2 of slab designed for 50 years of reliable service. This unit allows consistent comparison of environmental and social impacts. Preventive maintenance was included to support this lifespan. A "cradle-to-grave" scope covered raw material extraction, manufacturing, construction, use-phase maintenance, and End-of-Life (EoL) treatment, ensuring all relevant processes and impacts were systematically considered. All life cycle inventories and impact calculations were modeled using the Ecoinvent v3.2 database, in accordance with ISO 14040/44 and reported following EN 15804 reporting conventions: the system boundaries therefore include the product stage (A1–A3), transport to site and installation (A4–A5), the use stage limited to preventive maintenance activities (B – maintenance), and end-of-life processes (C – demolition, material recovery and final disposal). This explicit mapping to EN 15804 modules clarifies that the study goes beyond A1–A4 and represents a full cradle-to-grave assessment for the functional unit considered.

The manufacturing stage includes all material production processes and transport to the site, with transport distances estimated based on the average location of suppliers and production plants in major Argentine urban areas (City of Buenos Aires, Córdoba and La Plata), which correspond to the origin of the majority of case study buildings reported in Appendix B. Typical transport distances assumed in the model are: 5–10 km for ready-mix concrete (reflecting the proximity of batching plants to construction sites), 40–50 km for reinforcing steel and maintenance materials such as anti-carbonation paint (supplied from industrial zones in the urban periphery), 5–15 km for formwork (sourced from central urban warehouses), and 20–35 km for lightweight void fillers such as recycled HDPE and EPS (produced/recycled in suburban industrial areas). Construction covers machinery and onsite work for 1 m^2 of slab. Maintenance considers material production and transport, notably acrylic anti-carbonation paint transported 40–50 km, to ensure 50 years of service. The EoL phase involves concrete demolition, crushing, waste separation, and transport to recycling facilities at similar distances for concrete, steel, and recycled plastic. For conventional slabs with EPS, an extra 25 km of transport to the landfill is included for EPS disposal. These values are presented as realistic averages for urban Argentine contexts and were applied consistently across comparative scenarios; we acknowledge that transport assumptions can influence certain impact categories (e.g., fossil depletion and GWP) and this potential influence is discussed in the manuscript's Discussion section as a limitation and as a motivation for future sensitivity analyses.

The second phase involved inventory analysis using the widely accepted Ecoinvent 3.2 database, valued for its transparency and detailed classification of construction materials and processes. Table 2 summarizes materials with their Ecoinvent process equivalents for VS and CS. Machinery energy consumption data during construction and end-of-life stages came from the BEDEC database (Catalonia Institute of Construction Technology). Transport processes were modeled across all life cycle stages. The SOCA v2 database, compatible with Ecoinvent, supported social impact assessment, ensuring methodological consistency with environmental analyses.

In the third phase, OpenLCA software modeled life cycle processes to quantify environmental and social impacts. Data quality was assessed using the pedigree matrix—introduced by Weidema and Wesnæs (1996)—which evaluates reliability, completeness, and temporal, geographical, and technological correlation (Feng et al., 2022). These indicators assign uncertainty factors combined with a base value to calculate each dataset's lognormal standard deviation, enabling robust uncertainty propagation. However, SOCA provides extensive global social impact data, and incomplete country-specific details are required using global averages (Jiang et al., 2024).

The ReCiPe 2016 methodology (Huijbregts et al., 2017) assessed environmental impacts at both midpoint and endpoint levels. The midpoint approach provided detailed insights into 18 specific impact categories, offering a granular understanding of potential environmental burdens. These categories include: agricultural land occupation (ALO), global warming potential (GWP), fossil depletion (FD), freshwater ecotoxicity (FEPT), freshwater eutrophication (FEP), human toxicity (HTP), ionizing radiation (IRP), marine ecotoxicity (MEPT), marine eutrophication (MEP), metal depletion (MD), natural land transformation (NLT), ozone depletion (ODP), particulate matter formation (PMF), photochemical oxidant formation (POFP), terrestrial acidification (TAP), terrestrial ecotoxicity (TEPT), urban land occupation (ULO), and water depletion (WD). In parallel, the ReCiPe endpoint approach aggregated these into three broader damage categories: Human health, measured in disability-adjusted life years (DALYs); Ecosystems, quantified as species lost per year; and Resource availability, expressed in monetary terms (USD). A hierarchical (H) perspective was adopted, reflecting a long-term global policy context. Impact scores were normalized using the ReCiPe World H/H (person/year) methodology, enabling comparison across damage categories within a consistent framework.

The social impact assessment was conducted in accordance with the UNEP/SETAC (2009; 2013) Guidelines for Social Life Cycle Assessment. It utilized the SOCA database, which was developed as an extension of Ecoinvent v3.7.1, adapting the Product Social Impact Life Cycle Assessment (PSILCA) framework to Ecoinvent processes. This ensures complete methodological consistency with the environmental model, enabling the traceable quantification of social risks across the same supply chains. Four stakeholder groups were assessed—Workers, Local Communities, Society, and Value Chain Actors—each evaluated through 20 subcategories defined by SOCA and relevant to construction activities

Table 2
Processes included in the life cycle inventory.

Process	Unit	Ecoinvent process
Concrete[a, b]	m^3	Concrete, 25 MPa
Reinforcing steel[a, b]	kg	Reinforcing steel
HDPE discs or spheres[a]	kg	Polystyrene foam slab
EPS blocks[b]	kg	Blow moulding
Slab casting[a, b]	MJ	Diesel, burned in machine
Anti-carbonation paint[a, b]	kg	Epoxy resin
Demolition[a, b]	MJ	Diesel, burned in machine
Concrete crushing[a, b]	kg	Rock crushing

[a] VS.
[b] CS.

(Sánchez-Garrido et al., 2024). Workers include child and forced labor, fair wages, working hours, discrimination, health and safety, benefits, legal compliance, and freedom of association; Value Chain Actors cover fair competition, corruption, social responsibility, and conflict prevention; Society includes economic development and public health and safety; and Local Communities address access to resources, Indigenous rights, living conditions, local employment, migration, and environmental effects.

Social risks were quantified using the Mean Risk per Hour (MRH) indicator, as defined in the PSILCA and SOCA frameworks. MRH expresses the relative social risk associated with one working hour within a given process, based on sectoral and geographical labor statistics and social data. Each process in the life cycle inventory was linked to the corresponding labor-hour data within SOCA, ensuring that MRH values were derived directly from the activity levels modeled in OpenLCA. The resulting risk values were then aggregated by weighting each subcategory according to its share of total working hours within the respective stakeholder group and life cycle stage.

Since SOCA and Ecoinvent may not include country-specific datasets for Argentina, activities categorized under "Global (GLO)" or "Rest of World (RoW)" were systematically applied. These datasets represent either global average production or the remaining production share not covered by regional datasets, ensuring a comprehensive yet consistent representation of global supply chains. This approach aligns with the standard Ecoinvent system model, where RoW is dynamically generated to avoid overlaps with regional activities. The selection of social impact categories followed three criteria: (i) alignment with UNEP/SETAC guidelines, (ii) relevance to the construction sector, and (iii) data coverage within SOCA. This multi-criteria selection ensures transparency, reproducibility, and methodological coherence with international S-LCA practice. The overall approach provides a consistent framework for identifying social hotspots in construction supply chains and for comparing the performance of the Voided Slab (VS) and Conventional Slab (CS) systems.

3. Analysis of results

3.1. Multivariate analysis

The initial bivariate analysis yielded a Pearson correlation coefficient of 0.9076, indicating a strong linear relationship between slab thickness (t, in centimeters) and main span (L, in meters). A simple linear regression was performed using the least squares method at a 95 % confidence level. The resulting model (Eq. 1) explains approximately 82.4 % of the variability in t ($R^2 = 0.8237$). The Durbin–Watson test produced a p-value of 0.2992, indicating no significant autocorrelation in the residuals. Observations with standardized residuals exceeding ±2 are listed in Appendix B, Table B.4, suggesting potential outliers. One case showed a studentized residual greater than 3: a hotel with a 30 cm slab was deemed excessive for its span compared to similar cases. This outlier was retained, as the deviation likely reflects increased design loads due to building use, not a modeling error.

$$t = 1.48802 + (2.94598 \bullet L) \quad (1)$$

The multivariate analysis included sphere height (H_e, cm), characteristic live load (Q_1, kN/m^2), alternative live load (Q_2, kN/m^2), and the square of the span (L^2, m^2) as predictors. Correlation, covariance, and partial correlation analyses (Fig. 2) showed strong Pearson coefficients between slab thickness (t, cm) and L, H_e, and L^2, with a moderate correlation to Q_1, while Q_2 exhibited negligible correlation. The best-fitting model incorporated H_e, Q_1, and L^2, yielding $R^2 = 97.22$ % and adjusted $R^2 = 97.10$ %, demonstrating excellent explanatory power. The Durbin–Watson test ($p > 0.05$) indicated no autocorrelation, and ANOVA confirmed the model's overall significance at the 95 % confidence level

Table 3
Non-standardized coefficients of the adjusted model (Eq. 2).

Parameter	Estimation	Typical error	T	Significance
Constant	5.61245	0.4593	12.2195	0.0000
H_e (cm)	0.78093	0.04204	18.5768	0.0000
Q_1 (kN/m^2)	0.33568	0.14251	2.3553	0.0213
L^2 (m^2)	0.06044	0.00597	10.1277	0.0000

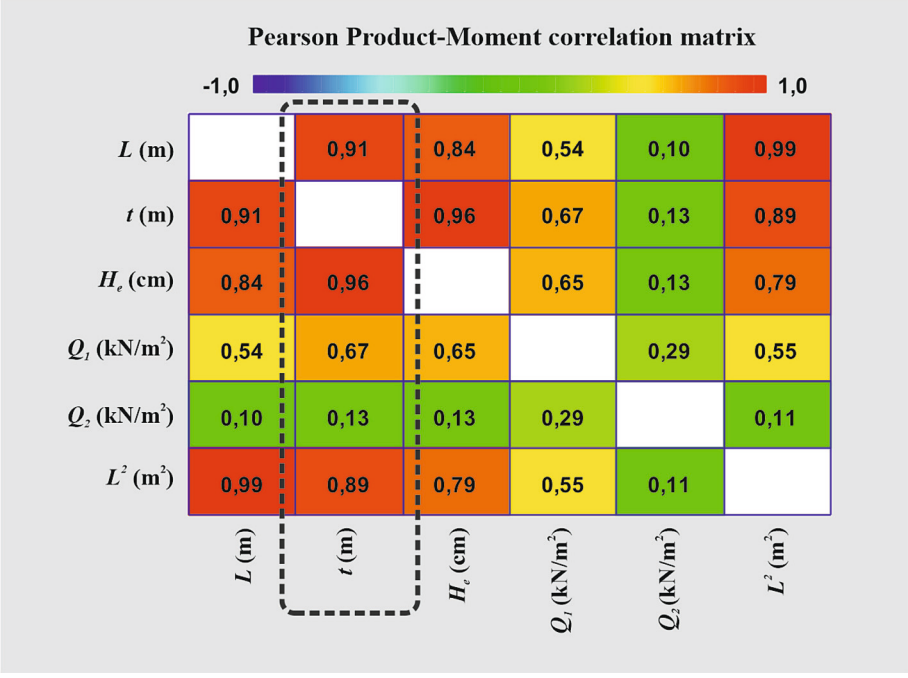

Fig. 2. Pearson correlation matrix between model variables.

($p < 0.05$).

Variable significance analysis (Table 3) showed all predictors retained statistical relevance, with the highest p-value of 0.0213 for Q_1, supporting their inclusion in the final model (Eq. 2). However, Table 4 reveals notable multicollinearity among predictors, with absolute correlation coefficients exceeding 0.5 (excluding the constant term). Residual analysis (Table B.4) identified atypical observations with studentized residuals >2: observations 4 and 5 (same building, different blocks), row 66 (single-family dwelling with an unusual span-to-thickness ratio), and row 70 (complex airport structure affecting normality assumptions). Overload values for these cases were adjusted. Observation 62 (office building) was excluded as an outlier due to requiring an unrealistically low overload to fit the model, which could distort results. Accepted observations showed no anomalies and were retained unchanged.

$$t = 5.61245 + (0.78093 \bullet H_e) + (0.33568 \bullet Q_1) + (0.06044 \bullet L^2) \quad (2)$$

After data cleaning, a third refined model was developed via multiple regression on the selected variables. The coefficient of determination ($R^2 = 98.34$ %) and adjusted R^2 (98.26 %) confirm strong explanatory power. The Durbin–Watson test yielded a p-value >0.05, indicating no significant autocorrelation in residuals at the 95 % confidence level and supporting residual independence. ANOVA results ($p < 0.05$) confirm a statistically significant relationship among variables. Table 5 summarizes the regression results, with Q_1 showing the highest significance yet below the 0.05 threshold; thus, all variables remain in the model (Eq. 3). Table 6 presents the correlation matrix of coefficient estimates. The value for H_e is valid, as slab thickness influences it. Although H_e shows multicollinearity, this is expected given the standard commercial heights of these elements, which must be known for design. Outliers with studentized residuals >2 are listed in Appendix B, Table B.5; none exceed an absolute value of 3.

$$t = 6.0064 + (0.7717 \bullet H_e) + (0.3679 \bullet Q_1) + (0.0553 \bullet L^2) \quad (3)$$

To enhance usability during preliminary design, Eq. 3 was simplified by replacing its decimal coefficients with nearby simple fractions (Eq. 4). The constant term (~6 cm) is a fixed concrete cover of 3 cm on each face to protect reinforcement and ensure durability. This cover is distinct from the structural thickness, which depends on core height, live load, and span. The quadratic term in L^2 is also reformulated as $(L/n)^2$, using a rational denominator ($\sqrt{18}$) that balances accuracy and ease of manual calculation. The resulting formula retains the original's precision with a conservative margin, improving its practical application.

$$t = 6 + \left(\frac{4}{5}H_e\right) + \left(\frac{2}{5}Q_1\right) + \left(L/\sqrt{18}\right)^2 \quad (4)$$

3.2. LCA and S-LCA

The statistical model was applied to a case study of low-seismic-hazard cities in Buenos Aires province, representing 55 of the 67 building cases analyzed (Table B.1). Eq. 1 selected an appropriate disc or sphere based on commercially available heights, then applied in the refined model (Eq. 3) to determine the VS thickness. Table 7 summarizes the material inventory for the VS and CS, considering column spans from 6 to 12 m. Compared to the CS, the VS achieves concrete savings from 23 % (9 m span) up to 33 % (6 m span), with steel reinforcement reduced by up to 29 % for 6 m spans. The VS incorporates up to 2.64 kg of recycled plastic discs or spheres per functional unit.

Table 4
Correlation matrix of the estimated coefficients of the adjusted model (Eq. 2).

–	Constant	H_e (cm)	Q_1 (kN/m^2)	L^2 (m^2)
Constant	1.0000	−0.7159	−0.0866	0.3634
H_e (cm)	−0.7159	1.0000	−0.4209	−0.6856
Q_1 (kN/m^2)	−0.0866	−0.4209	1.0000	−0.0726
L^2 (m^2)	0.3634	−0.6856	−0.0726	1.0000

Table 5
Non-standardized coefficients of the refined model (Eq. 3).

Parameter	Estimation	Typical error	T	Significance
Constant	6.006	0.3355	17.9052	0.0000
H_e (cm)	0.772	0.0309	24.9945	0.0000
Q_1 (kN/m^2)	0.368	0.1103	3.3339	0.0014
L^2 (m^2)	0.055	0.0045	12.1679	0.0000

Table 6
Correlation matrix of the estimated coefficients of the refined model (Eq. 3).

–	Constant	H_e (cm)	Q_1 (kN/m^2)	L^2 (m^2)
Constant	1.0000	−0.6671	−0.1273	0.3003
H_e (cm)	−0.6671	1.0000	−0.4497	−0.6900
Q_1 (kN/m^2)	−0.1273	−0.4497	1.0000	0.0043
L^2 (m^2)	0.3003	−0.6900	0.0043	1.0000

Energy consumption associated with machinery operations during construction and End-of-Life was obtained from the BEDEC database (December 2024 update). The applied energy coefficients for concreting and demolition processes are reported in Appendix C, together with the calculated energy values per 1 m^2 of slab for the representative 12 m span.

The inventory was modeled in OpenLCA, where Ecoinvent v3.2 provides detailed input and output flows for each process. As illustration, Appendix C presents the energy-related input flows for the main materials—concrete, reinforcing steel, and recycled plastic void formers. In cases where country-specific datasets were unavailable, Rest of World (RoW) processes were consistently applied. Data quality and uncertainty were managed using the pedigree matrix, assessing reliability, completeness, and temporal, geographical, and technological correlation; the corresponding matrix for the main modeled processes is also presented in Appendix C.

Midpoint environmental impacts for the 1 m^2 functional unit of the VS were quantified and compared to the CS across 18 categories. To enhance transparency, the emission values for the main materials (concrete, reinforcing steel, and void formers) are presented in Appendix C for the 12 m span case of both VS and CS. Although the categories offer detailed insights, their different units and scales complicate interpretation. The 12-m slab was selected as a representative. Fig. 3 shows normalized results, setting CS values at 100 % in 17 categories. VS significantly reduces most impacts, with fossil depletion and photochemical oxidant formation potential decreasing by 29 % and 28 %, respectively. Water depletion shows the most minor reduction (17 %), while agricultural land occupation is the only category where VS scores 100 %, and CS is 28 % lower. This results from Ecoinvent's attribution of agricultural land use to plastics—even recycled ones—due to biomass-derived feedstocks, unlike mineral-based materials.

Given the critical role of CO_2 emissions in global warming, Fig. 4 presents a detailed GWP analysis in three parts. Subfigure (a) shows total CO_2 emissions (kg), with VS reducing emissions by an average of 24 % compared to CS, reaching a maximum 30 % reduction at a 6 m span. Subfigure (b) breaks down process contributions, identifying concrete production as the largest emitter (53.5 % for VS, 55.8 % for CS), followed by steel. Plastic discs or spheres contribute only 4.1 %, but their recycled nature enhances environmental benefits. Subfigure (c) details emissions by life cycle stage, with manufacturing having the most significant impact. The EoL stage represents 7.1 % (VS) and 7.4 % (CS), covering demolition and recycling pretreatment that enable material reuse.

The final results, summarized in Fig. 5, aggregate environmental impacts into three damage categories—Ecosystems, Human Health, and Resources—to facilitate interpretation and comprehensively assess the

Table 7
Life cycle inventory data by functional unit and span length for voided and conventional slabs.

Process	6 m	7 m	8 m	9 m	10 m	11 m	12 m	Unit
Lightweight voided slab (VS) with pressurized recycled plastic discs or spheres								
Concrete slab, 25 MPa	0.13	0.14	0.18	0.20	0.21	0.24	0.25	m^3
Reinforcing steel B500S	11.25	12.78	16.02	18.09	18.99	21.24	22.14	kg
HDPE discs or spheres	1.98	3.20	2.42	3.20	3.20	2.64	2.64	kg
Concrete slab pouring	18.17	20.65	25.88	29.22	30.68	34.31	35.77	MJ/m^3
Carbonation-resistant coating	0.40	0.40	0.40	0.40	0.40	0.40	0.40	kg
Concrete slab demolition	33.42	37.96	47.58	53.73	56.41	63.09	65.76	MJ/m^3
Concrete waste crushing	280.61	318.78	399.59	451.22	473.67	529.80	552.24	kg
Conventional slab (CS)								
Concrete slab, 25 MPa	0.19	0.20	0.24	0.26	0.29	0.32	0.35	m^3
Reinforcing steel B500S	15.84	16.42	20.16	20.96	23.71	24.68	28.09	kg
EPS blocks	0.99	1.01	1.20	1.48	1.35	1.54	1.81	kg
Concrete slab pouring	26.96	29.02	34.63	38.09	42.40	45.91	50.52	MJ/m^3
Carbonation-resistant coating	0.20	0.20	0.21	0.20	0.22	0.22	0.22	kg
Concrete slab demolition	49.57	53.37	63.67	70.04	77.96	84.41	92.88	MJ/m^3
Concrete waste crushing	416.29	448.16	534.63	588.16	654.63	708.83	779.98	kg

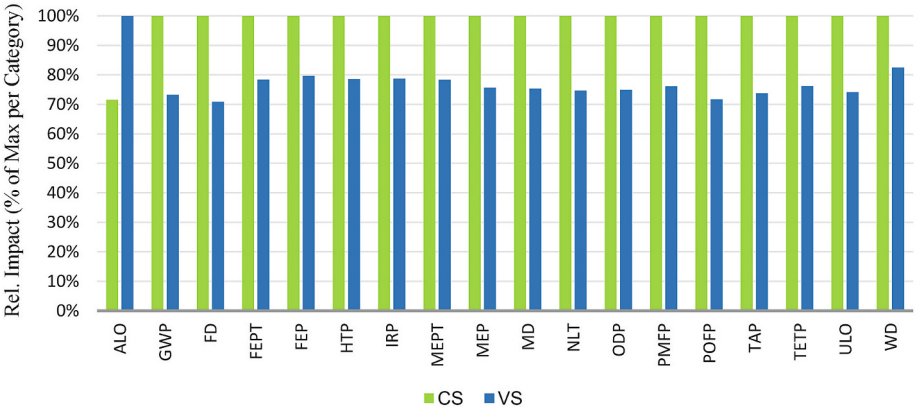

Fig. 3. Normalized comparison of midpoint environmental impacts for a 12 m slab span.

overall environmental burden. The VS exhibits reductions of up to 26 % in ecosystem impact for the 6-m span and decreases of up to 29 % in the Human Health category. The most significant improvements occur in the Resources category, with reductions ranging from 22 % (9-m span) to 31 % (6-m span). Subfigure (d) presents the total normalized final scores, where the VS consistently demonstrates lower environmental impacts across all spans, averaging a 25 % overall reduction.

The social impacts assessed through S-LCA are summarized in Fig. 6. For both slab types, the highest impacts occur in the Workers and Society categories. Within the Workers category, workload-related factors—including social security contributions, union expenses, and child labor risks—constitute 77 % of the impact for the VS and 75 % for the CS. In the Society category, lack of education predominates, accounting for 76 % of the impact in both cases. These patterns reflect the structure of the global construction supply chain, where labor intensity and limited access to education or training contribute to higher social risks.

The VS system mitigates these pressures by lowering material demand and simplifying on-site operations, which translates into fewer work hours, reduced exposure to occupational hazards, and improved safety conditions. The selection and evaluation of social impact categories followed the UNEP/SETAC (2009; 2013) guidelines and the SOCA v2 framework, ensuring consistency across life cycle stages. MRH values were calculated automatically within OpenLCA using the activity levels modeled for each process and weighted according to the share of labor hours in each stakeholder group.

The most significant reductions in social impact for the VS compared to the CS are observed in the Local Community and Workers categories, with decreases of 20 % and 19 %, respectively, for the 6-m span. This improvement mainly arises from reduced on-site labor, fewer heavy material movements, and shorter project durations. The most minor reductions occur at the 9-m span, limited by the commercial height availability of the spheres used in the VS design. Overall, the S-LCA results confirm that material-efficient structural innovations can generate measurable social co-benefits—particularly in occupational safety and local community well-being—reinforcing the multidimensional sustainability of voided slab systems.

4. Discussion

This study introduces an innovative MMC structural system: a beamless, bidirectional flat slab lightened with recycled plastic spheres or discs. Preliminary design guidance was derived from multivariate data analysis on 67 real buildings. Environmental and social benefits were assessed through LCA and S-LCA, benchmarked against a CS. Resting directly on columns, the VS system enables simplified formwork, faster execution, and reduced building height for the same usable area (Nicácio et al., 2020). However, adoption remains limited due to structural design uncertainties, the lack of dedicated codes, and scarce environmental and social performance data.

The refined model in Eq. 3 estimates VS thickness using a minimal variable set from 67 real buildings. The Durbin–Watson test confirmed no residual autocorrelation at 95 % confidence (Jin et al., 2018). The

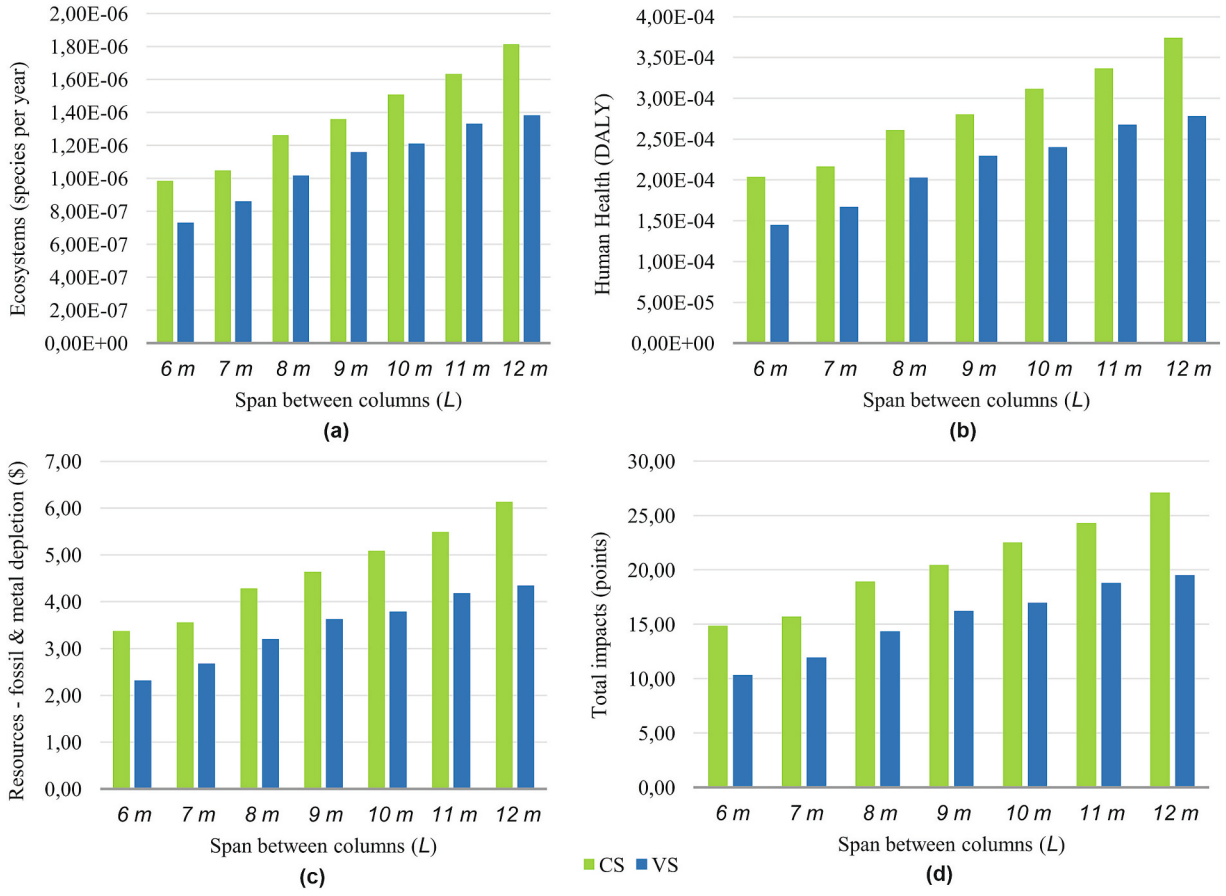

Fig. 4. CO_2 Emissions by span (a), process (b), and LCA stage (c).

adjusted R^2 of 98.26 % indicates an excellent fit. To further address potential concerns of overfitting, predictive accuracy was quantified using the Mean Absolute Error (MAE) and the Root Mean Square Error (RMSE). The obtained values (MAE = 1.15 cm; RMSE = 2.57 cm) are low relative to the slab thickness range (16–42 cm), representing about 4–10 % of the average thickness. These values confirm that the regression model achieves reliable predictions suitable for preliminary slab design. Standardized residuals remained within ±3, indicating no significant outliers. Homoscedasticity was validated through the Residuals vs. Predicted plot (Fig. 7), which shows no systematic trends and stable variance around zero.

Ensuring an unrestricted applicability range between L and t is crucial for the preliminary design's validity across all structures. This requires residuals to follow a Normal distribution, evaluated via a standard probability plot against a uniform probability plot. As illustrated in Fig. 8, residuals exhibit the expected Normal pattern without extreme values, confirming the model's statistical robustness after outlier removal and readjustment.

Residuals were evaluated for Normality, showing a mean near zero (−0.0007142), indicating centered residuals. The Shapiro–Wilk test (statistic = 0.987, $p = 0.69$) and Kolmogorov–Smirnov test (minimum $p = 0.75$) both support Normality at 95 % confidence. Table 8 compares distributions fitted to residuals; although the logistic distribution had the best log-likelihood, its curve closely overlaps with the Normal distribution, as shown in Fig. 9. These results confirm residual Normality, validating the refined model in Eq. 3.

Research on innovative slab systems has focused mainly on structural performance—flexural behavior, shear strength, and seismic resistance—while environmental impact assessments remain scarce (Paik and Na, 2019b). Comprehensive comparisons of environmental performance are limited, and social impacts are largely unexplored. Using global databases like Ecoinvent improves data accessibility, consistency, and comparability, aiding decision-makers in evaluating construction material impacts (Li et al., 2025). Midpoint indicators offer a detailed characterization of environmental mechanisms, enabling more precise source identification and involving less uncertainty than endpoints due to fewer modeling assumptions.

Endpoint impact results offer a broad overview of environmental performance by enabling direct comparisons across categories, though they involve greater uncertainty due to complex modeling. This study found a 25 % total endpoint environmental impact reduction for VS compared to CS. Specifically, the VS system achieves an average 24 % CO_2 reduction, aligning with previous findings. Paik and Na (2019a) reported a 15 % CO_2 decrease for hollow core slabs versus traditional reinforced concrete slabs over the life cycle. Paik and Na (2019b) observed a 34 % CO_2 reduction for VS compared to CS, considering raw material extraction, transportation, and manufacturing.

S-LCA has advanced notably in the last decade, yet the construction sector lacks standardized methodologies, causing social impacts to be often overlooked or inadequately assessed (Backes and Traverso, 2024). This challenge echoes broader trends identified in sustainability and urban vulnerability research, where the absence of harmonized frameworks has similarly limited comprehensive assessment (Salas and Yepes, 2018). Challenges include limited data, selection and interpretation of social indicators, addressing positive and negative impacts, absence of standardized codes, and complex stakeholder analysis (Dong et al., 2023). This study used the SOCA database, which integrates PSILCA social data and aligns with Ecoinvent processes by assigning corresponding social impacts, enabling efficient reuse of environmental LCA models. The social impact categories follow Benoît et al. (2010), ensuring methodological consistency. Employing identical process models for environmental and social assessments enhances result

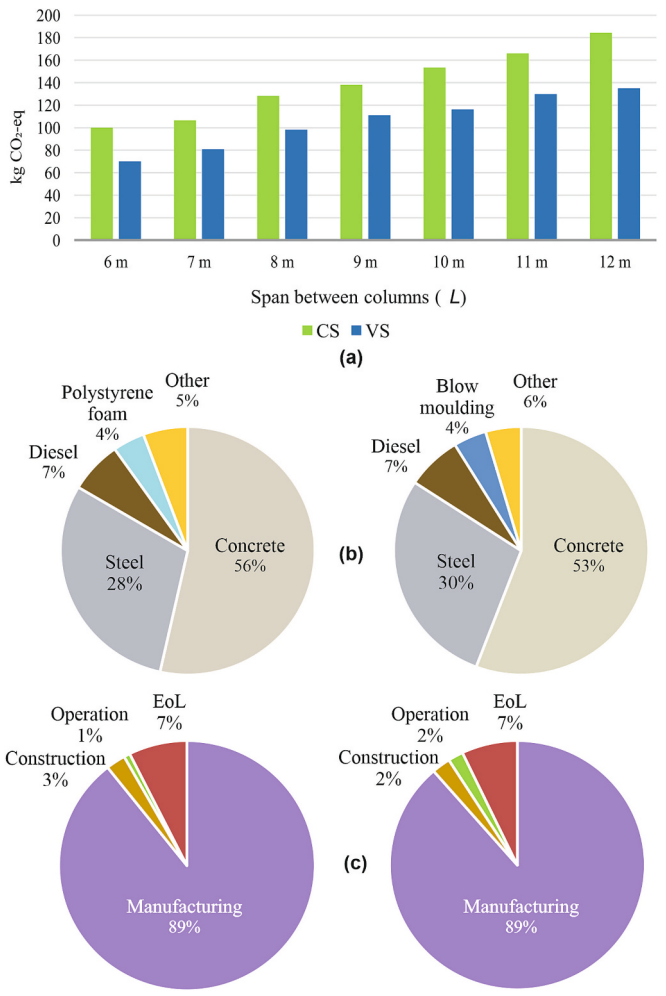

Fig. 5. Endpoint Environmental Impacts: Ecosystems (a), Human Health (b), Resources (c), and total score (d).

coherence and comparability (Penadés-Plà et al., 2020).

Although this research integrates environmental and social assessments, the economic dimension could not be addressed through life-cycle cost analysis (LCCA) due to the lack of detailed cost data in the case study context. This omission is explicitly recognized as a limitation, since cost considerations are decisive for technology adoption and market diffusion. Future studies should therefore extend the framework to include LCCA, enabling a comprehensive triple-bottom-line sustainability assessment of voided slab systems.

Similarly, since the functional unit was defined as 1 m^2 of slab, the analysis does not directly capture per capita implications by housing typology (e.g., detached houses, mid-rise or high-rise residential). We acknowledge this as a limitation and highlight that future applications of the framework could integrate LCA results with demographic and occupancy data to quantify per capita impacts across building types.

The VS system's discs and spheres use recycled HDPE from post-consumer waste recovered from oceans and landfills (Ferdous et al., 2021), addressing major environmental threats. This aligns with circular

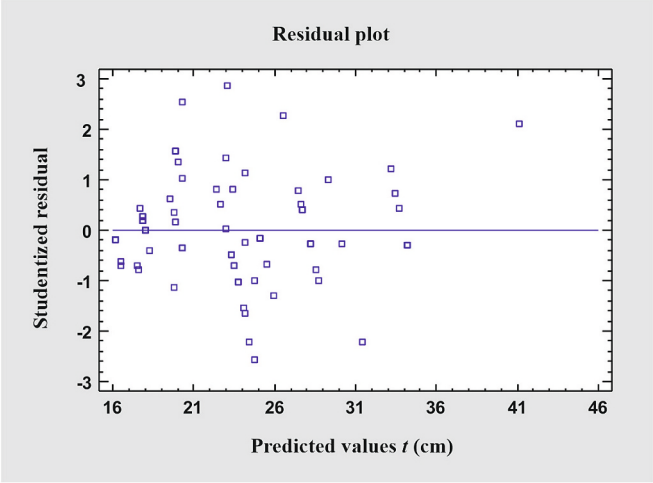

Fig. 7. Homoscedasticity check: residuals vs. estimated t (cm).

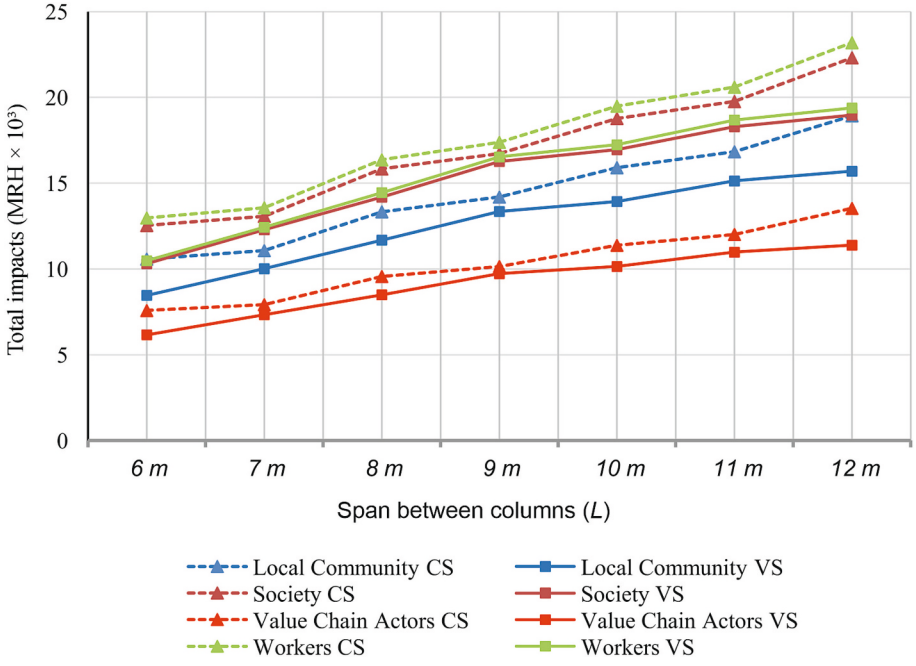

Fig. 6. Social impacts categorized by S-LCA stakeholders.

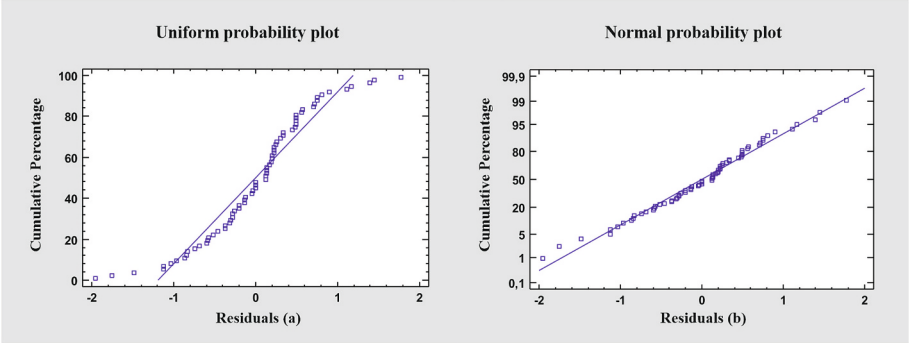

Fig. 8. Residual probability plots comparing Uniform (a) and Normal (b) distributions.

Table 8
Comparison of candidate probability distributions.

Distribution	Metrics	Log-likelihood	KSD
Logistics	2	−75.039	0.0777
Normal	2	−75.5161	0.0811
Laplace	2	−75.9223	0.09415
Min Extreme Value	2	−79.421	0.102043
Max Extreme Value	2	−84.2289	0.122859
Uniform	2	−92.336	0.1922
Inverse Gaussian	2	−92.336	–
Pareto	1	−1.00E+09	0.9889
Loglogistic	2	−1.00E+09	0.4857
Exponential	1	−7.00E+10	–
Lognormal	2	−7.00E+10	0.4857
Welbull	2	−7.00E+10	0.4857
Gamma	2	−7.00E+10	–
Birnbaum-saunders	Unadjusted	–	–

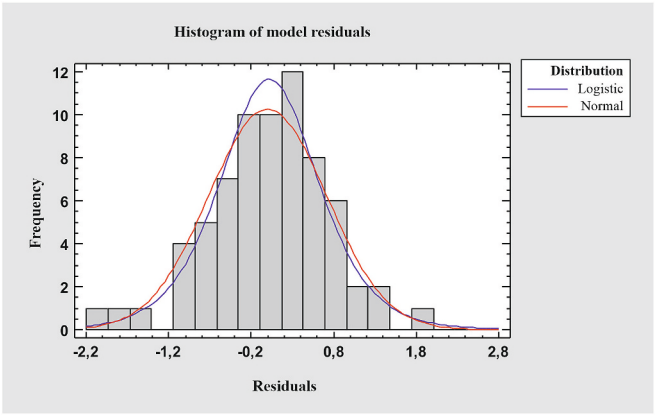

Fig. 9. Histogram of residuals with logistic and normal distribution fits.

economy principles by repurposing waste as lightweight void formers within the slab. Although standards estimate a 50-year service life (Ministry of Transport, Mobility and Urban Agenda, 2021), many structures exceed 70–80 years with proper maintenance (Sánchez-Garrido et al., 2026), keeping the recycled plastic encapsulated for decades and removing it from pollution cycles. This long-term immobilization reduces virgin material use and mitigates marine and terrestrial plastic pollution, increasing recycled HDPE's environmental and economic value (Yang et al., 2025). However, further research is needed to evaluate its long-term behavior and durability within concrete to ensure structural and environmental stability.

Adopting a CE approach is increasingly vital to meeting the SDGs. In concrete production, this involves using waste materials or industrial by-products. However, clear guidelines are needed to evaluate trade-offs—such as those linked to recycled plastic discs or spheres in VS systems (Li et al., 2022). Integrating circularity indicators is key to operationalizing these principles. Plastic waste management remains globally problematic due to limited recycling infrastructure and environmental harm. Incorporating plastic waste into concrete offers a promising solution by reducing waste volume and increasing the economic value of recycled materials (Haigh, 2025). Benefits include lower waste management and construction material costs, as plastic waste is abundant and economically viable to reuse. Several countries facing high plastic pollution are implementing programs and funding mechanisms to support industrial reuse (Da Silva et al., 2021). Within this context, the present framework contributes to strengthening the empirical understanding of material stocks. It flows within the built environment by quantifying material intensity, substitution potential, and embodied impacts at the structural component level. By translating these data into measurable reductions in concrete and steel demand, the study provides boundary conditions and parameters that can be integrated into larger-scale material flow analyses and urban metabolism models. This linkage between micro-scale (component) evidence and macro-scale resource modeling enhances the systemic understanding of construction-sector decarbonization, helping to ensure that mitigation efforts are coherent, data-driven, and effectively targeted rather than fragmented.

Importantly, the PRENOVA database underlying this study covers 75 slab typologies across a broad spectrum of real residential projects, from single-family houses to mid-rise apartment blocks and high-rise towers (Appendix B, Table B.2). These appendices were deliberately included to ensure complete transparency of the empirical basis, allowing readers and future researchers to verify representativeness and, if desired, to stratify environmental impacts by building typology. To better connect the structural and sustainability analyses with spatial planning practice, the 67 case studies were stratified according to the spatial typology defined in Table B.2. Approximately 25 % of the buildings correspond to Rural/Suburban environments, 40 % to urban, and 35 % to high-density urban contexts. Average slab thickness and span show a consistent increase with built density—from about 19 cm and 6.8 m in Rural/Suburban buildings to 30 cm and 9.5 m in High-Density Urban ones—indicating that material demand intensifies with construction density. This gradient provides a quantitative proxy of material intensity across spatial forms, demonstrating that denser urban typologies accumulate disproportionately larger material stocks per unit area. Consequently, the environmental and social advantages of the voided slab system are most pronounced in high-density urban contexts, where each incremental reduction in concrete or steel consumption yields amplified system-level benefits in terms of embodied energy and emissions. The spatial stratification, therefore, provides an interpretive lens for linking structural efficiency with land-use intensity, supporting planners and policymakers in targeting circular construction measures where their impact is maximized—namely, dense, resource-intensive urban areas.

Incorporating recycled plastic spheres or discs into VS systems

continues to spark debate over allocating environmental impacts from concrete by-products, as no consensus has been reached (Sánchez-Garrido et al., 2024). A major obstacle to broader adoption is the absence of standardized construction regulations for recycled plastic use. Current applications depend largely on R&D rather than formal codes, with limited processing or long-term performance guidance, constraining commercial viability (Da Silva et al., 2021). The environmental benefits of plastic waste circularity as a by-product remain uncertain. While this study's LCA excluded such benefits, it recognizes their potential to reduce resource depletion through avoided waste. Given the complexity of LCA under decarbonization and CE strategies, some simplifying assumptions are necessary. Excluding the recycled plastic burden, the VS system shows an average 27 % CO_2 emissions reduction compared to conventional slabs.

VS technology has recently attracted interest in reducing material consumption without compromising structural integrity. Current research emphasizes optimizing void geometry and layout to enhance slab performance. Advances in manufacturing and design have improved precision and consistency in void formation, boosting both efficiency and environmental benefits (Ingeli et al., 2025).

From an environmental management perspective, the findings of this study provide valuable insights for policy and regulatory frameworks. The demonstrated reductions in concrete and steel demand, alongside lower social risks, suggest that circular slab systems could be promoted through green public procurement, the integration of recycled content requirements into building codes, and financial incentives for circular construction materials. Embedding such measures into policy instruments would not only accelerate the market adoption of voided slab systems but also align construction practices with national decarbonization pathways and the Sustainable Development Goals (SDGs), in line with recent evidence on effective policy strategies for advancing circular construction (Ding et al., 2025).

Although the study offers robust comparative insights, certain methodological aspects help to contextualize the results and indicate promising directions for future work. Applying the cut-off allocation method for recycled plastics follows established recommendations to avoid overburdening secondary materials (Visintin et al., 2020). However, complementary sensitivity analyses with alternative rules could provide additional evidence of robustness (Gravina et al., 2021). Likewise, the exclusion of life-cycle cost assessment reflects a common barrier in sustainability studies of MMC systems, where the absence of reliable cost data constrains comprehensive triple-bottom-line evaluations (Hernández et al., 2023; Patrisia et al., 2025). Another limitation stems from the intrinsic uncertainty of LCA modeling—linked to background databases, regional variability, and characterization methods (Huijbregts et al., 2017; Feng et al., 2022)—which advises caution when interpreting absolute values, even though relative comparisons remain consistent. Finally, while the PRENOVA dataset documents 75 slab typologies across diverse residential projects and ensures transparency, further applications to non-residential or regionally distinct practices would enhance the external validity and generalizability of the findings.

5. Conclusions

The construction industry, while a cornerstone of the global economy, remains a substantial driver of environmental degradation due to its intensive resource consumption and high CO_2 emissions. In accelerating urbanization, embedding CE principles into construction practices is imperative to mitigate the sector's ecological footprint substantially. This study contributes to this critical transition by proposing and rigorously validating an innovative MMC: a reinforced concrete biaxial VS system incorporating 100 % recycled, pressurized plastic spheres or discs as void formers. Despite their clear environmental and technical potential, the adoption of VS technology is hindered by the absence of explicit regulatory frameworks and comprehensive sustainability assessments that integrate environmental and social dimensions.

To overcome these challenges, this work develops statistically robust slab thickness pre-dimensioning guidelines derived from multivariate analysis of empirical data collected from 67 real-world buildings. The resulting model demonstrates exceptional predictive accuracy (adjusted $R^2 = 98.26$ %), with diagnostic tests confirming the absence of autocorrelation and homoscedasticity, thereby validating its applicability across diverse structural scenarios. Key explanatory variables—sphere height, squared span length, and primary live load—were identified as statistically significant determinants of slab thickness, collectively explaining variability with high precision. This optimized modeling framework enables more efficient structural design processes by accelerating preliminary decision-making and reducing overall design time without compromising safety or performance.

E-LCA reveals a substantial reduction in the ecological footprint of voided slabs relative to conventional solid slabs, with endpoint indicators averaging a 25 % decrease and global warming potential showing a mean reduction of 24 %, reaching up to 30 % for a typical six-meter span slabs. These reductions primarily reflect decreased concrete volumes enabled by the voided geometry, as cement production and manufacturing remain the dominant contributors to overall environmental impact. While the recycled plastic spheres or discs impart a marginal environmental burden, their inclusion exemplifies CE principles by valorizing plastic waste streams and promoting resource recirculation.

S-LCA further highlights notable benefits, particularly in the "Local Community" and "Workers" categories, with impact reductions up to 20 % and 19 %, respectively, indicating improved occupational health, safety, and reduced social disruptions. The integrated assessment framework ensures methodological consistency, allowing comprehensive evaluation of the system's multidimensional sustainability profile. However, quantifying circularity benefits—especially regarding the environmental allocation of concrete by-products—remains a contentious issue, reflecting the current lack of methodological consensus and underscoring the urgent need for standardized approaches in this domain.

In summary, this innovative MMC significantly advances circular construction by demonstrating empirically substantiated environmental and social advantages. Nevertheless, the absence of tailored regulations and limited quantification of comparative benefits pose critical barriers to widespread adoption. By integrating empirical structural data with comprehensive environmental and social LCA, this study furnishes a rigorous evidence base to inform future design guidelines, regulatory frameworks, and policy-making to promote resource-efficient, circular construction aligned with global sustainability objectives. It should also be noted that the dataset is primarily composed of projects located in Argentina (63 out of 67 cases), with four additional cases from Uruguay, Bolivia, and Armenia. As a result, the findings largely reflect Argentine construction practices and electricity grid conditions, and validation with local data would be required before extrapolating these results to other regional contexts.

Declaration of competing interest

The authors whose names are listed immediately below certify that they have NO affiliations with or involvement in any organization or entity with any financial interest (such as honoraria; educational grants; participation in speakers' bureaus; membership, employment, consultancies, stock ownership, or other equity interest; and expert testimony or patent-licensing arrangements), or non-financial interest (such as personal or professional relationships, affiliations, knowledge or beliefs) in the subject matter or materials discussed in this manuscript.

Acknowledgments

Grant PID2023-150003OB-I00 funded by MICIU/AEI/10.13039/501100011033 and by "ERDF/EU".

We sincerely thank Ricardo Levinton, CEO of Prenova System S.L., for providing essential data and information that greatly contributed to this study.

Appendix A. List of abbreviations and acronyms used in the study

ALO	- Agricultural Land Occupation
ANOVA	- Analysis of Variance
BEDEC	- Banco Estructurado de Datos de Elementos Constructivos
BIM	- Building Information Modeling
CE	- Circular Economy
CO_2	- Carbon Dioxide
CS	- Conventional Slab
C.V.	- Coefficient of Variation
DALYs	- Disability-Adjusted Life Years
Durbin–Watson	- Test for autocorrelation in regression residuals
Ecoinvent	- International Database for Life Cycle Inventory Data
EoL	- End-of-Life
EPS	- Expanded Polystyrene
FD	- Fossil Depletion
FEPT	- Freshwater Ecotoxicity
FEP	- Freshwater Eutrophication
GWP	- Global Warming Potential
HDPE	- High-Density Polyethylene
HTP	- Human Toxicity Potential
IRP	- Ionizing Radiation Potential
KSD	- Kolmogorov–Smirnov Distance
LCA	- Life Cycle Assessment
LCCA	- Life Cycle Cost Assessment
MD	- Metal Depletion
MEP	- Marine Eutrophication Potential
MEPT	- Marine Ecotoxicity Potential
MMC	- Modern Methods of Construction
MRH	- Mean Risk per Hour
NLT	- Natural Land Transformation
ODP	- Ozone Depletion Potential
OpenLCA	- Software for life cycle impact assessment modeling
PMF	- Particulate Matter Formation
POFP	- Photochemical Oxidant Formation Potential
PRENOVA	- Commercial name of voided slab system with recycled plastic
PSILCA	- Product Social Impact Life Cycle Assessment database
R&D	- Research and Development
ReCiPe	- Harmonized LCIA methodology at midpoint/endpoint level
S-LCA	- Social Life Cycle Assessment
SDGs	- Sustainable Development Goals
Shapiro–Wilk	- Test for normality of residuals
SOCA	- Social Organizational Capacity Assessment Database
Statgraphics	- Software used for multivariate analysis and regression
TAP	- Terrestrial Acidification Potential
TEPT	- Terrestrial Ecotoxicity
ULO	- Urban Land Occupation
USD	- United States Dollar
VS	- Voided Slab
WD	- Water Depletion

Appendix B. Case study database of voided slabs (PRENOVA)

Table B.1
Dataset comprising 67 buildings and 75 observation units.

Ref.	Project and executed work	Location	ID
BLD 001	Vacani Building (teleCentro)	Lomas de Mirador, Buenos Aires, Argentina	1
BLD 002	Casagrande	José Ignacio, Uruguay	2 3
BLD 003	Dolores Judicial Complex	Dolores, Buenos Aires, Argentina	4
BLD 004	Olavarría Judicial Complex	Olavarría, Buenos Aires, Argentina	5
BLD 005	Don Bosco Residence	Quilmes, Buenos Aires, Argentina	6
BLD 006	Residence in Santa Fe	Santa Fe, Santa Fe, Argentina	7
BLD 007	Álamos de los Andes Complex	San Martín de los Andes, Neuquén, Argentina	8
BLD 008	Villa Traful Environmental Interpretation Center	Villa Traful, Neuquén, Argentina	9
BLD 009	La Palmera Building (ground floor extension)	Olivos, Buenos Aires, Argentina	10

(*continued on next page*)

Table B.1 (*continued*)

Ref.	Project and executed work	Location	ID
BLD 010	Building in Lanús	Lanús, Autonomous City of Buenos Aires, Argentina	11
BLD 011	Li Residence	Mar del Plata, Buenos Aires, Argentina	12
BLD 012	Chateau del Portal	Nordelta, Buenos Aires, Argentina	13
BLD 013	Residence in Mar del Plata	Mar del Plata, Buenos Aires, Argentina	14
BLD 014	Mandel 3 Building – Santa Fe	Santa Fe, Argentina	15
BLD 015	Florencia Condominium	Santa Cruz de la Sierra, Bolivia	16
BLD 016	Boulevard Alcorta Building (2545 Av. Alcorta)	Moreno, Buenos Aires, Argentina	17
BLD 017	Céspedes Building	Céspedes 3645, Autonomous City of Buenos Aires, Argentina	18
BLD 018	Franklin Building	Franklin 1212, Autonomous City of Buenos Aires, Argentina	19
BLD 019	Guardia Vieja Building	Guardia Vieja 3757, Aut.City of Buenos Aires, Argentina	20
BLD 020	Italia and Albarellos Building	Tigre, Buenos Aires, Argentina	21 22
BLD 021	Jaramillo Building	Jaramillo 2937, Autonomous City of Buenos Aires, Argentina	23
BLD 022	José Hernández Building	José Hernández 2222, Aut. City of Buenos Aires, Argentina	24
BLD 023	Lisandro de la Torre Building	Lisandro de la Torre 3294, Santa Fe, Argentina	25
BLD 024	Jacinto Chiclana Building	Moreno, Buenos Aires, Argentina	26
BLD 025	"La Diva" Tower Building	Córdoba, Argentina	27 28 29
BLD 026	Santa María de Tigre Offices	Rincón de Milberg, Buenos Aires, Argentina	30
BLD 027	Ribera Studios	San Isidro, Buenos Aires, Argentina	31
BLD 028	Serena Parque San Martín Building	Mar del Plata, Buenos Aires, Argentina	32
BLD 029	Stockcenter	San Isidro, Buenos Aires, Argentina	33
BLD 030	Cagnone Residence	Chivilcoy, Buenos Aires, Argentina	34
BLD 031	Cavadini Residence	Chivilcoy, Buenos Aires, Argentina	35 36
BLD 032	San Diego Residence	Moreno, Buenos Aires, Argentina	37
BLD 033	Windbells Residence	San Fernando, Buenos Aires, Argentina	38
BLD 034	Johnson & Son Offices	San Isidro, Buenos Aires, Argentina	39
BLD 035	New Terminals – Ezeiza Airport	Ezeiza, Buenos Aires, Argentina	40
BLD 036	Libertador 650 Offices	Vicente López, Buenos Aires, Argentina	41 42
BLD 037	Grand Brizo La Plata Hotel 5*	La Plata, Buenos Aires, Argentina	43 44
BLD 038	K41 Business Complex	Moreno, Buenos Aires, Argentina	45
BLD 039	Alma de Agua Complex	Federación, Buenos Aires, Argentina	46
BLD 040	Forbes Offices	–	47
BLD 041	Campos Salles Building	Campos Salles 2025, Aut. City of Buenos Aires, Argentina	48
BLD 042	Guayra Building	Guayra 1848, Autonomous City of Buenos Aires, Argentina	49
BLD 043	Las Heras Building	Mar del Plata, Buenos Aires, Argentina	50
BLD 044	Tapiales Building	Tapiales 1129, Olivos, Buenos Aires, Argentina	51
BLD 045	Quetzal Bio	San Nicolás, Buenos Aires, Argentina	52
BLD 046	San Francisco Residence	Manzanares, Buenos Aires, Argentina	53
BLD 047	Serena V Building	Mar del Plata, Buenos Aires, Argentina	54
BLD 048	El Encuentro Residence	Bancalari, Buenos Aires, Argentina	55
BLD 049	Ancón Building	Ancón 5353, Autonomous City of Buenos Aires, Argentina	56
BLD 050	Av. Patricios Building	Av. Patricios 265, Autonomous City of Buenos Aires, Argentina	57
BLD 051	Manuela Pedraza Building	Manuela Pedraza 3286, Aut. City of Buenos Aires, Argentina	58
BLD 052	Proa Building	Vicente López, Buenos Aire, Argentina	59
BLD 053	September 11 Offices	September 11, Autonomous City of Buenos Aires, Argentina	60
BLD 054	Guido Offices (more like residential floors)	Guido 1933, Autonomous City of Buenos Aires, Argentina	61
BLD 055	OSECAC Building	Arenales 1569, Autonomous City of Buenos Aires, Argentina	62
BLD 056	Vilela Building	Autonomous City of Buenos Aires, Argentina	63
BLD 057	Arismendi Building	Arismendi 2360, Autonomous City of Buenos Aires, Argentina	64
BLD 058	Milberg Residence	Jacarandá Nhd, Rincón de Milberg, Tigre, Buenos Aires, Argentina	65 66
BLD 059	Martínez Residence	Martínez, Buenos Aires, Argentina	67
BLD 060	Zapiola Building	Zapiola 3625, Autonomous City of Buenos Aires, Argentina	68
BLD 061	Nordelta Residence	Golf Club Neighborhood, Nordelta, Buenos Aires, Argentina	69
BLD 062	Zvartnots Airport	Yerevan, Armenia	70
BLD 063	Milberg Offices	Rincón de Milberg Neighborhood, Buenos Aires, Argentina	71
BLD 064	Malabia Commercial Space	Malabia 1683, Autonomous City of Buenos Aires, Argentina	72
BLD 065	"O" Building	Parada 7, La Brava, Punta del Este, Uruguay	73
BLD 066	Santiago del Estero Courthouse	Santiago del Estero, Argentina	74
BLD 067	La Lucila Residence	Roma 1113, La Lucila, Buenos Aires, Argentina	75

Table B.2
Observations — 75 types of studied voided slabs (PRENOVA).

ID	L (m)	t (cm)	H_e (cm)	Q_1 (kN/m^2)	Q_2 (kN/m^2)	Slab area (m^2)	Year	Building use	No. floors	Spatial typology
1	9.00	34	27	5.00	4.00	4000	2018	Industrial building	G + 3	Urban
2	7.00	21	14	2.00	3.00	6000	2018	Hotel building	G + 2 + P	High-Density Urban
3	7.00	30	27	5.00	–					
4	12.00	40	27	5.00	3.00	15,000	2017	Courthouse	G + 2	High-Density Urban
5	12.00	40	27	5.00	3.00	11,000	2017	Courthouse	G + 3	High-Density Urban
6	6.50	21	14	2.00	1.00	160	2016	Single-family house	G + 1 + RH	Rural / Suburban
7	7.50	23	17	2.00	1.00	210	2016	Single-family house	G + 1	Rural / Suburban
8	5.50	16	10	2.00	1.00	2658	2015	Apartment building	G + 2	Urban
9	5.90	18	12	3.00	4.00	330	2015	Office building	G	Rural / Suburban
10	10.00	34	27	5.00	3.00	1400	2015	Commercial building	G + 1	Urban
11	5.70	18	12	2.00	3.00	715	2015	Apartment building	G + 4	Urban
12	5.70	18	12	2.00	1.00	341	2014	Single-family house	G + 1	Rural/Suburban
13	6.50	21	14	2.00	3.00	9600	2014	Apartment building	B + 2G + 2 + RH	High-Density Urban
14	6.50	20	14	2.00	1.00	380	2014	Single-family house	G + 1	Rural/Suburban
15	6.00	18	12	2.00	3.00	1478	2014	Apartment building	G + 7	Urban
16	8.00	23	18	2.00	3.00	8.800	2013	Apartment building	G + 7	High-Density Urban
17	6.50	20	14	3.00	4.00	1407	2013	Office building	2G + 5	Urban
18	5.50	16	10	2.00		700	2013	Single-family house	G + 2 + P	Rural/Suburban
19	6.00	18	12	2.00	3.00	1550	2013	Apartment building	G + 3	Urban
20	7.00	20	14	2.00	3.00	1900	2013	Apartment building	G + M + 1 + P	Urban
21	5.20	17	12	2.00	3.00	6500	2013	Apartment building	G + 6	High-Density Urban
22	6.70	21	14							
23	8.50	28	22	2.00	3.00	1100	2013	Apartment building	G + 3 + RH	Urban
24	5.20	16	10	2.00	3.00	6500	2013	Apartment building	G + 8	High-Density Urban
25	5.50	18	12	2.00	4.00	2600	2013	Apartment building	G + 2 + 9	High-Density Urban
26	5.50	16	10	2.00	3.00	3000	2013	Apartment building	G + 5	Urban
27	6.40	19	14	2.00	3.00	31,000	2013	Apartment building	G + 21	High-Density Urban
28	8.00	24	17					Apartment building	G + 2	
29	10.20	34	27	3.00	4.00			Office building		
30	7.50	23	18	3.00	4.00	1590	2013	Office building	G + 2	Urban
31	9.50	28	22	2.00	3.00	4800	2013	Apartment building	B + G + 2 + RH	Urban
32	7.00	23	18	2.00	3.00	5800	2013	Apartment building	G + 13 + RH	High-Density Urban
33	10.00	34	27	5.00		978	2013	Commercial building	G + 1?	Urban
34	7.50	23	18	2.00	1.00	735	2013	Single-family house	G + 1	Rural/Suburban
35	6.00	18	12	2.00	1.00	265	2013	Single-family house	G + 1	Rural/Suburban
36	9.00	28	22							
37	9.00	28	22	2.00	1.00	609	2013	Single-family house	G	Rural/Suburban
38	6.80	23	17	2.00	1.00	700	2013	Single-family house	G + 1	Rural/Suburban
39	10.50	30	22	3.00	4.00	17,880	2012	Office building	G + 3	High-Density Urban
40	10.00	34	27	5.00	–	18,160	2012	Airport terminal	B + G + 2	High-Density Urban
41	8.00	28	22	3.00	4.00	2782	2012	Office building	26	High-Density Urban
42	9.00	30	22	5.00	3.00				G + 1	
43	8.50	28	22	2.00	3.00	10,563	2012	Hotel building	11	High-Density Urban
44	15.00	42	27	5.00	?				2G + MEP + PS	
45	10.00	34	27	3.00	4.00	17,050	2012	Office building	2G + 2 + P	High-Density Urban
46	6.00	16	10	2.00	3.00	5050	2012	Apartment building	G + 3	High-Density Urban
47	8.20	24	18	3.00	4.00	2650	2012	Office building	2G + 9	High-Density Urban
48	6.50	22	14	2.00	3.00	3090	2012	Apartment building	G + 4 + RH	Urban
49	6.00	20	14	2.00	3.00	1550	2012	Apartment building	G + 3	Urban
50	7.20	23	18	2.00	3.00	8500	2012	Apartment building	G + 10 + RH	High-Density Urban
51	5.80	18	12	2.00	3.00	965	2012	Apartment building	G + 4	Urban
52	5.30	17	12	2.00	3.00	1750	2012	Apartment building	G + 6	Urban
53	7.50	23	18	2.00	1.00	380	2012	Single-family house	G + 1	Rural/Suburban
54	6.30	20	14	2.00	3.00	1631	2011	Apartment building	G + 6	Urban
55	6.50	24	18	2.00	1.00	750	2011	Single-family house	G + 1	Rural/Suburban
56	7.00	23	18	2.00	3.00	1441	2011	Apartment building	G + 9	High-Density Urban
57	7.20	23	18	2.00	–	3220	2011	Apartment building	G + 10	High-Density Urban
58	5.80	18	12	2.00	–	1050	2011	Apartment building	G + 3	Urban
59	9.00	28	22	3.00	4.00	12,000	2010	Office building	G + 15	High-Density Urban
60	8.66	23	18	3.00	4.00	1660	2010	Office building	G + 3	Urban
61	5.50	16	10	3.00	2.00	2300	2010	Office building	G + 8	High-Density Urban
62	9.00	23	18	3.00	4.00	1980	2010	Office building	G + 4	Urban
63	8.00	25	18	2.00	3.00	1400	2010	Apartment building	G + 3 + P	Urban
64	6.60	25	18	2.00	3.00	1246	2010	Apartment building	G + 6	Urban
65	9.76	25	18	2.00	1.00	175	2010	Single-family house	G + 1	Rural/Suburban
65	9.00	23	18	2.00	1.00	3000	2009	Single-family house	G + 1	Urban
66	9.00	28	21	2.00	3.00	505	2009	Apartment building	G + 3	Rural/Suburban
67	6.00	23	18							
68	9.00	25	18	2.00	1.00	300	2009	Single-family house	G + 1	Rural/Suburban
69	8.00	23	18	5.00		45,000	2008	Airport terminal	S + G + 2	High-Density Urban
70	9.00	25	18	3.00	4.00	3000	2008	Office building	G + 2	Urban
71	6.66	28	21	5.00	1.00	237	2007	Commercial building	2G + 1	Rural/Suburban
72	8.00	24	18	2.00	3.00	10,500	2006	Apartment building	S + G + 10	High-Density Urban

(*continued on next page*)

Table B.2 (*continued*)

ID	L (m)	t (cm)	H_e (cm)	Q_1 (kN/m^2)	Q_2 (kN/m^2)	Slab area (m^2)	Year	Building use	No. floors	Spatial typology
73	7.00	23	18	5.00	3.00	15,000	2006	Courthouse	G + 6 + RH	High-Density Urban
74	9.00	25	18	2.00	1.00	300	2006	Single-family house	SB + G + 1	Rural/Suburban
75	5.80	18	12	2.00	3.00	965	2012	Apartment building	G + 4	Urban

Codes for building levels: B = Basement; SB = Semi-basement; PS = Public square slab; G = Ground floor; 2G = Double-height ground floor; M = Mezzanine; MEP = Mechanical/plant floor; P = Penthouse; RH = Rooftop headhouse.

Spatial Typology classification: This classification integrates vertical (number of floors) and horizontal (slab area) indicators to approximate built density and land-use intensity:

- Rural/Suburban – low-rise (≤2 floors) and small footprint (<1000 m^2).
- Urban – mid-rise (3–7 floors) or medium footprint (1000–5000 m^2).
- High-Density Urban – high-rise (≥8 floors) or large footprint (>5000 m^2).

This combined criterion better reflects the material intensity and functional scale of each case, avoiding misclassification of extensive low-rise facilities such as airports or industrial complexes.

Table B.3
Dataset overview > STATGRAPHICS Initial model results (Eq. 1)*.

Ref.	L (m)	t (cm)	H_e (cm)	Q_1 (kN/m^2)	Q_2 (kN/m^2)	L^2 (m^2)	t* (cm)
1	9.00	34	27	5.00	4.00	81.00	28.00
2	7.00	21	14	2.00	3.00	49.00	22.11
3	7.00	30	27	5.00	–	49.00	22.11
4	12.00	40	27	5.00	3.00	144.00	36.84
5	12.00	40	27	5.00	3.00	144.00	36.84
6	6.50	21	14	2.00	1.00	42.25	20.64
7	7.50	23	17	2.00	1.00	56.25	23.58
8	5.50	16	10	2.00	1.00	30.25	17.69
9	5.90	18	12	3.00	4.00	34.81	18.87
10	10.00	34	27	5.00	3.00	100.00	30.95
11	5.70	18	12	2.00	3.00	32.49	18.28
12	5.70	18	12	2.00	1.00	32.49	18.28
13	6.50	21	14	2.00	3.00	42.25	20.64
14	6.50	20	14	2.00	1.00	42.25	20.64
15	6.00	18	12	2.00	3.00	36.00	19.16
16	8.00	23	18	2.00	3.00	64.00	25.06
17	6.50	20	14	3.00	4.00	42.25	20.64
18	5.50	16	10	2.00	–	30.25	17.69
19	6.00	18	12	2.00	3.00	36.00	19.16
20	7.00	20	14	2.00	3.00	49.00	22.11
21	5.20	17	12	2.00	3.00	27.04	16.81
22	6.70	21	14	2.00	3.00	44.89	21.23
23	8.50	28	22	2.00	3.00	72.25	26.53
24	5.20	16	10	2.00	3.00	27.04	16.81
25	5.50	18	12	2.00	4.00	30.25	17.69
26	5.50	16	10	2.00	3.00	30.25	17.69
27	6.40	19	14	2.00	3.00	40.96	20.34
28	8.00	24	17	2.00	3.00	64.00	25.06
29	10.20	34	27	3.00	4.00	104.04	31.54
30	7.50	23	18	3.00	4.00	56.25	23.58
31	9.50	28	22	2.00	3.00	90.25	29.47
32	7.00	23	18	2.00	3.00	49.00	22.11
33	10.00	34	27	5.00	–	100.00	30.95
34	7.50	23	18	2.00	1.00	56.25	23.58
35	6.00	18	12	2.00	1.00	36.00	19.16
36	9.00	28	22	2.00	1.00	81.00	28.00
37	9.00	28	22	2.00	1.00	81.00	28.00
38	6.80	23	17	2.00	1.00	46.24	21.52
39	10.50	30	22	3.00	4.00	110.25	32.42
40	10.00	34	27	5.00		100.00	30.95
41	8.00	28	22	3.00	4.00	64.00	25.06
42	9.00	30	22	5.00	3.00	81.00	28.00
43	8.50	28	22	2.00	3.00	72.25	26.53
44	15.00	42	27	5.00	–	225.00	45.68
45	10.00	34	27	3.00	4.00	100.00	30.95
46	6.00	16	10	2.00	3.00	36.00	19.16
47	8.20	24	18	3.00	4.00	67.24	25.65
48	6.50	22	14	2.00	3.00	42.25	20.64
49	6.00	20	14	2.00	3.00	36.00	19.16
50	7.20	23	18	2.00	3.00	51.84	22.70
51	5.80	18	12	2.00	3.00	33.64	18.57
52	5.30	17	12	2.00	3.00	28.09	17.10
53	7.50	23	18	2.00	1.00	56.25	23.58

(*continued on next page*)

Table B.3 (*continued*)

Ref.	L (m)	t (cm)	H_e (cm)	Q_1 (kN/m^2)	Q_2 (kN/m^2)	L^2 (m^2)	t^* (cm)
54	6.30	20	14	2.00	3.00	39.69	20.05
55	6.50	24	18	2.00	1.00	42.25	20.64
56	7.00	23	18	2.00	3.00	49.00	22.11
57	7.20	23	18	2.00	–	51.84	22.70
58	5.80	18	12	2.00	–	33.64	18.57
59	9.00	28	22	3.00	4.00	81.00	28.00
60	8.66	23	18	3.00	4.00	75.00	27.00
61	5.50	16	10	3.00	2.00	30.25	17.69
62	9.00	23	18	3.00	4.00	81.00	28.00
63	8.00	25	18	2.00	3.00	64.00	25.06
64	6.60	25	18	2.00	3.00	43.56	20.93
65	9.76	25	18	2.00	1.00	95.26	30.24
66	9.00	23	18	2.00	1.00	81.00	28.00
67	9.00	28	21	2.00	1.00	81.00	28.00
68	6.00	23	18	2.00	3.00	36.00	19.16
69	9.00	25	18	2.00	1.00	81.00	28.00
70	8.00	23	18	5.00	–	64.00	25.06
71	9.00	25	18	3.00	4.00	81.00	28.00
72	6.66	28	21	5.00	1.00	44.36	21.11
73	8.00	24	18	2.00	3.00	64.00	25.06
74	7.00	23	18	5.00	3.00	49.00	22.11
75	9.00	25	18	2.00	1.00	81.00	28.00

Note: t is slab thickness adapted to void formers; t^* is model-predicted thickness.

Table B.4
Dataset overview > STATGRAPHICS Adjusted model results (Eq. 2)*.

Ref.	L (m)	t (cm)	H_e (cm)	Q_1 (kN/m^2)	Q_2 (kN/m^2)	L^2 (m^2)	t^* (cm)	*Residuals*
1	9.00	34	27	5.00	4.00	81.00	33.27	−0.73
2	7.00	21	14	2.00	3.00	49.00	20.18	−0.82
3	7.00	30	27	5.00	–	49.00	31.34	1.34
4 (X)	12.00	40	27	5.00	3.00	144.00	37.08	−2.92
5 (X)	12.00	40	27	5.00	3.00	144.00	37.08	−2.92
6	6.50	21	14	2.00	1.00	42.25	19.77	−1.23
7	7.50	23	17	2.00	1.00	56.25	22.96	−0.04
8	5.50	16	10	2.00	1.00	30.25	15.92	−0.08
9	5.90	18	12	3.00	4.00	34.81	18.09	0.09
10	10.00	34	27	5.00	3.00	100.00	34.42	0.42
11	5.70	18	12	2.00	3.00	32.49	17.62	−0.38
12	5.70	18	12	2.00	1.00	32.49	17.62	−0.38
13	6.50	21	14	2.00	3.00	42.25	19.77	−1.23
14	6.50	20	14	2.00	1.00	42.25	19.77	−0.23
15	6.00	18	12	2.00	3.00	36.00	17.83	−0.17
16	8.00	23	18	2.00	3.00	64.00	24.21	1.21
17	6.50	20	14	3.00	4.00	42.25	20.11	0.11
18	5.50	16	10	2.00	–	30.25	15.92	−0.08
19	6.00	18	12	2.00	3.00	36.00	17.83	−0.17
20	7.00	20	14	2.00	3.00	49.00	20.18	0.18
21	5.20	17	12	2.00	3.00	27.04	17.29	0.29
22	6.70	21	14	2.00	3.00	44.89	19.93	−1.07
23	8.50	28	22	2.00	3.00	72.25	27.83	−0.17
24	5.20	16	10	2.00	3.00	27.04	15.73	−0.27
25	5.50	18	12	2.00	4.00	30.25	17.48	−0.52
26	5.50	16	10	2.00	3.00	30.25	15.92	−0.08
27	6.40	19	14	2.00	3.00	40.96	19.69	0.69
28	8.00	24	17	2.00	3.00	64.00	23.43	−0.57
29	10.20	34	27	3.00	4.00	104.04	33.99	−0.01
30	7.50	23	18	3.00	4.00	56.25	24.08	1.08
31	9.50	28	22	2.00	3.00	90.25	28.92	0.92
32	7.00	23	18	2.00	3.00	49.00	23.30	0.30
33	10.00	34	27	5.00	–	100.00	34.42	0.42
34	7.50	23	18	2.00	1.00	56.25	23.74	0.74
35	6.00	18	12	2.00	1.00	36.00	17.83	−0.17
36	9.00	28	22	2.00	1.00	81.00	28.36	0.36
37	9.00	28	22	2.00	1.00	81.00	28.36	0.36
38	6.80	23	17	2.00	1.00	46.24	22.35	−0.65
39	10.50	30	22	3.00	4.00	110.25	30.46	0.46
40	10.00	34	27	5.00	–	100.00	34.42	0.42
41	8.00	28	22	3.00	4.00	64.00	27.67	−0.33
42	9.00	30	22	5.00	3.00	81.00	29.37	−0.63
43	8.50	28	22	2.00	3.00	72.25	27.83	−0.17
44	15.00	42	27	5.00	–	225.00	41.98	−0.02
45	10.00	34	27	3.00	4.00	100.00	33.75	−0.25
46	6.00	16	10	2.00	3.00	36.00	16.27	0.27

(*continued on next page*)

Table B.4 (*continued*)

Ref.	L (m)	t (cm)	H_e (cm)	Q_1 (kN/m^2)	Q_2 (kN/m^2)	L^2 (m^2)	t^* (cm)	*Residuals*
47	8.20	24	18	3.00	4.00	67.24	24.74	0.74
48 (A)	6.50	22	14	2.00	3.00	42.25	19.77	−2.23
49	6.00	20	14	2.00	3.00	36.00	19.39	−0.61
50	7.20	23	18	2.00	3.00	51.84	23.47	0.47
51	5.80	18	12	2.00	3.00	33.64	17.69	−0.31
52	5.30	17	12	2.00	3.00	28.09	17.35	0.35
53	7.50	23	18	2.00	1.00	56.25	23.74	0.74
54	6.30	20	14	2.00	3.00	39.69	19.62	−0.38
55	6.50	24	18	2.00	1.00	42.25	22.89	−1.11
56	7.00	23	18	2.00	3.00	49.00	23.30	0.30
57	7.20	23	18	2.00	–	51.84	23.47	0.47
58	5.80	18	12	2.00	–	33.64	17.69	−0.31
59	9.00	28	22	3.00	4.00	81.00	28.70	0.70
60 (R)	8.66	23	18	3.00	4.00	75.00	25.21	2.21
61	5.50	16	10	3.00	2.00	30.25	16.26	0.26
62 (R)	9.00	23	18	3.00	4.00	81.00	25.57	2.57
63	8.00	25	18	2.00	3.00	64.00	24.21	−0.79
64 (A)	6.60	25	18	2.00	3.00	43.56	22.97	−2.03
65	9.76	25	18	2.00	1.00	95.26	26.10	1.10
66 (X)	9.00	23	18	2.00	1.00	81.00	25.24	2.24
67	9.00	28	21	2.00	1.00	81.00	27.58	−0.42
68	6.00	23	18	2.00	3.00	36.00	22.52	−0.48
69	9.00	25	18	2.00	1.00	81.00	25.24	0.24
70 (X)	8.00	23	18	5.00	–	64.00	25.22	2.22
71	9.00	25	18	3.00	4.00	81.00	25.57	0.57
72	6.66	28	21	5.00	1.00	44.36	26.37	−1.63
73	8.00	24	18	2.00	3.00	64.00	24.21	0.21
74	7.00	23	18	5.00	3.00	49.00	24.31	1.31
75	9.00	25	18	2.00	1.00	81.00	25.24	0.24

Notes: t is slab thickness adapted to void formers; t^* is model-predicted thickness.
A = Accept: Values within expected range and acceptable residuals, indicating good model fit.
R = Review: Values with moderate deviations or residuals, requiring further analysis.
X = Reject: Values with significant residuals or outliers, suggesting possible errors or exclusion.

Table B.5
Dataset overview > STATGRAPHICS Final model results (Eq. 3)*.

Ref.	L (m)	t (cm)	H_e (cm)	Q_1 (kN/m^2)	Q_2 (kN/m^2)	L^2 (m^2)	t^* (cm)	*Residuals*
1	9.00	34	27	5.00	4.00	81.00	33.16	−0.84
2	7.00	21	14	2.00	3.00	49.00	20.26	−0.74
3	7.00	30	27	5.00	–	49.00	31.39	1.39
4 (X)								
5 (X)								
6	6.50	21	14	2.00	1.00	42.25	19.88	−1.12
7	7.50	23	17	2.00	1.00	56.25	22.97	−0.03
8	5.50	16	10	2.00	1.00	30.25	16.13	0.13
9	5.90	18	12	3.00	4.00	34.81	18.30	0.30
10	10.00	34	27	5.00	3.00	100.00	34.22	0.22
11	5.70	18	12	2.00	3.00	32.49	17.80	−0.20
12	5.70	18	12	2.00	1.00	32.49	17.80	−0.20
13	6.50	21	14	2.00	3.00	42.25	19.88	−1.12
14	6.50	20	14	2.00	1.00	42.25	19.88	−0.12
15	6.00	18	12	2.00	3.00	36.00	18.00	0.00
16	8.00	23	18	2.00	3.00	64.00	24.17	1.17
17	6.50	20	14	3.00	4.00	42.25	20.25	0.25
18	5.50	16	10	2.00	–	30.25	16.13	0.13
19	6.00	18	12	2.00	3.00	36.00	18.00	0.00
20	7.00	20	14	2.00	3.00	49.00	20.26	0.26
21	5.20	17	12	2.00	3.00	27.04	17.50	0.50
22	6.70	21	14	2.00	3.00	44.89	20.03	−0.97
23	8.50	28	22	2.00	3.00	72.25	27.72	−0.28
24	5.20	16	10	2.00	3.00	27.04	15.96	−0.04
25	5.50	18	12	2.00	4.00	30.25	17.68	−0.32
26	5.50	16	10	2.00	3.00	30.25	16.13	0.13
27	6.40	19	14	2.00	3.00	40.96	19.81	0.81
28	8.00	24	17	2.00	3.00	64.00	23.40	−0.60
29	10.20	34	27	3.00	4.00	104.04	33.70	−0.30
30	7.50	23	18	3.00	4.00	56.25	24.11	1.11
31	9.50	28	22	2.00	3.00	90.25	28.71	0.71
32	7.00	23	18	2.00	3.00	49.00	23.34	0.34
33	10.00	34	27	5.00	–	100.00	34.22	0.22
34	7.50	23	18	2.00	1.00	56.25	23.75	0.75

(*continued on next page*)

Table B.5 (*continued*)

Ref.	L (m)	t (cm)	H_e (cm)	Q_1 (kN/m^2)	Q_2 (kN/m^2)	L^2 (m^2)	t^* (cm)	*Residuals*
35	6.00	18	12	2.00	1.00	36.00	18.00	0.00
36	9.00	28	22	2.00	1.00	81.00	28.20	0.20
37	9.00	28	22	2.00	1.00	81.00	28.20	0.20
38	6.80	23	17	2.00	1.00	46.24	22.42	−0.58
39	10.50	30	22	3.00	4.00	110.25	30.19	0.19
40	10.00	34	27	5.00	–	100.00	34.22	0.22
41	8.00	28	22	3.00	4.00	64.00	27.63	−0.37
42	9.00	30	22	5.00	3.00	81.00	29.31	−0.69
43	8.50	28	22	2.00	3.00	72.25	27.72	−0.28
44	15.00	42	27	5.00	–	225.00	41.13	−0.87
45	10.00	34	27	3.00	4.00	100.00	33.48	−0.52
46	6.00	16	10	2.00	3.00	36.00	16.45	0.45
47	8.20	24	18	3.00	4.00	67.24	24.72	0.72
48	6.50	22	14	3.00	2.00	42.25	20.25	−1.75
49	6.00	20	14	2.00	3.00	36.00	19.54	−0.46
50	7.20	23	18	2.00	3.00	51.84	23.50	0.50
51	5.80	18	12	2.00	3.00	33.64	17.86	−0.14
52	5.30	17	12	2.00	3.00	28.09	17.56	0.56
53	7.50	23	18	2.00	1.00	56.25	23.75	0.75
54	6.30	20	14	2.00	3.00	39.69	19.74	−0.26
55	6.50	24	18	2.00	1.00	42.25	22.97	−1.03
56	7.00	23	18	2.00	3.00	49.00	23.34	0.34
57	7.20	23	18	2.00	–	51.84	23.50	0.50
58	5.80	18	12	2.00	–	33.64	17.86	−0.14
59	9.00	28	22	3.00	4.00	81.00	28.57	0.57
60 (A*)	8.66	23	18	2.00	3.00	75.00	24.78	1.78
61	5.50	16	10	3.00	2.00	30.25	16.50	0.50
62 (X*)								
63	8.00	25	18	2.00	3.00	64.00	24.17	−0.83
64	6.60	25	18	2.00	3.00	43.56	23.04	−1.96
65	9.76	25	18	2.00	1.00	95.26	25.90	0.90
66 (X)								
67	9.00	28	21	2.00	1.00	81.00	27.43	−0.57
68	6.00	23	18	2.00	3.00	36.00	22.63	−0.37
69	9.00	25	18	2.00	1.00	81.00	25.12	0.12
70 (X)								
71	9.00	25	18	3.00	4.00	81.00	25.48	0.48
72	6.66	28	21	5.00	1.00	44.36	26.51	−1.49
73	8.00	24	18	2.00	3.00	64.00	24.17	0.17
74	7.00	23	18	5.00	3.00	49.00	24.45	1.45
75	9.00	25	18	2.00	1.00	81.00	25.12	0.12

Notes: t is slab thickness adapted to void formers; t^* is model-predicted thickness.
A* = Reinstated: Previously reviewed values now within acceptable range and residuals, indicating good model fit.
X* = Dismissed: Values previously under review but ultimately rejected due to poor fit or significant residuals.
X = Reject: Values initially rejected due to significant residuals or outliers, suggesting errors or exclusion.

Appendix C. Supplementary information

Table C.1
Primary energy coefficients of processes.

Process	Coefficient[a] (MJ/m^3)	VS (MJ/m^2)	CS (MJ/m^2)
Concrete slab casting	145.39	35.77	50.52
Demolition	267.33	65.76	92.88

[a] Source: BEDEC database, update December 2024.

Table C.2
Energy flow coefficients for key processes[a].

Energy flow	Unit	VS – Concrete (25 MPa)	VS – Reinforcing steel	VS – HDPE blow moulding (void formers)	CS – Concrete (25 MPa)	CS – Reinforcing steel	CS – EPS blocks (void formers)
Energy, geothermal, converted	MJ	0.6466	0.3811	0.1262	0.9052	0.4837	0.0382
Energy, gross calorific value, in biomass	MJ	6.8241	5.8663	12.0267	9.5537	7.4455	1.2065
Energy, gross calorific value, in biomass, primary forest	MJ	0.0057	0.0075	0.0046	0.0080	0.0096	0.0004

(*continued on next page*)

Table C.2 (*continued*)

Energy flow	Unit	VS – Concrete (25 MPa)	VS – Reinforcing steel	VS – HDPE blow moulding (void formers)	CS – Concrete (25 MPa)	CS – Reinforcing steel	CS – EPS blocks (void formers)
Energy, kinetic (in wind), converted	MJ	2.4619	2.9501	0.7148	3.4467	3.7442	0.3613
Energy, potential (in hydropower reservoir), converted	MJ	13.9374	13.7173	3.2538	19.5124	17.4100	1.4353
Energy, solar, converted	MJ	0.0248	0.0353	0.0003	0.0347	0.0448	0.0006

[a] Data source: Ecoinvent v3.2. Values expressed per functional unit of 1 m^2 of slab with a 12 m span.

Table C.3
Midpoint emissions by material[a].

Impact category	Unit	VS – Concrete (25 MPa)	VS – Reinforcing steel	VS – HDPE blow moulding (void formers)	CS – Concrete (25 MPa)	CS – Reinforcing steel	CS – EPS blocks (void formers)
Agricultural land occupation	m^2·a	0.9246	0.8084	1.7348	1.2944	1.0261	0.1219
Climate change	kg CO_2 eq	73.9560	41.0246	3.9783	103.5384	52.0683	7.8983
Fossil depletion	kg oil eq	9.2613	10.2580	1.1309	12.9658	13.0194	3.9629
Freshwater ecotoxicity	kg 1,4-dB eq	0.6415	1.3572	0.0585	0.8980	1.7225	0.0325
Freshwater eutrophication	kg P eq	0.0094	0.0196	0.0017	0.0131	0.0248	0.0009
Human toxicity	kg 1,4-dB eq	9.9066	16.6237	1.2702	13.8693	21.0987	0.6406
Ionizing radiation	kg U235 eq	2.2723	1.9128	0.3819	3.1813	2.4277	0.1999
Marine ecotoxicity	kg 1,4-dB eq	0.5811	1.3115	0.0523	0.8136	1.6645	0.0302
Marine eutrophication	kg N eq	0.0093	0.0120	0.0009	0.0130	0.0152	0.0009
Metal depletion	kg Fe eq	0.0047	0.0055	0.0012	0.0065	0.0070	0.0022
Natural land transformation	m^2	0.0150	0.0066	0.0006	0.0210	0.0084	0.0002
Ozone depletion	kg CFC-11 eq	2.83×10^{-6}	2.19×10^{-6}	1.11×10^{-7}	3.97×10^{-6}	2.78×10^{-6}	1.82×10^{-7}
Particulate matter formation	kg PM10 eq	0.0827	0.1156	0.0104	0.1158	0.1467	0.0096
Photochemical oxidant formation	kg NMVOC	0.2013	0.1952	0.0116	0.2819	0.2477	0.0444
Terrestrial acidification	kg SO_2 eq	0.1744	0.1331	0.0155	0.2441	0.1689	0.0260
Terrestrial ecotoxicity	kg 1,4-dB eq	0.0034	0.0024	0.0005	0.0047	0.0030	0.0003
Urban land occupation	m^2·a	2.4326	0.9701	0.0451	3.4056	1.2312	0.0218
Water depletion	m^3	112.6907	107.3314	26.8906	157.7670	136.2246	7.9907

[a] Data source: Ecoinvent v3.2. Values expressed per functional unit of 1 m^2 of slab with a 12 m span.

Table C.4
Uncertainty treatment: Ecoinvent pedigree matrix[a].

Ecoinvent process	VS – Concrete (25 MPa)	VS – Reinforcing steel	VS – HDPE blow moulding (void formers)	CS – Concrete (25 MPa)	CS – Reinforcing steel	CS – EPS blocks (void formers)
Reliability	1	1	1	1	1	1
Completeness	4	2	2	4	2	2
Temporal correlation	1	1	1	1	1	1
Geographical correlation	5	5	5	5	5	5
Technological correlation	2	2	2	2	2	2

[a] Base uncertainty coefficient: 1.05; Scales follow Ecoinvent pedigree matrix criteria: 1 = very good, 5 = very poor.

Data availability

Data will be made available on request.

References

Al-Gasham, T.S., Hilo, A.N., Alawsi, M.A., 2019. Structural behavior of reinforced concrete one-way slabs voided by polystyrene balls. Case Stud. Construct. Mater. 11, e00292. https://doi.org/10.1016/j.cscm.2019.e00292.

Amoushahi Khouzani, M., Zeynalian, M., Hashemi, M., Mostofinejad, D., Farahbod, F., 2020. Study on shear behavior and capacity of biaxial ellipsoidal voided slabs. Structures 27, 1075–1085. https://doi.org/10.1016/j.istruc.2020.07.017.

Backes, J.G., Traverso, M., 2024. Social life cycle assessment in the construction industry: systematic literature review and identification of relevant social indicators for carbon reinforced concrete. Environ. Dev. Sustain. 26 (3), 7199–7233. https://doi.org/10.1007/s10668-023-03005-6.

Barbhuiya, S., Das, B.B., Adak, D., 2024. A comprehensive review on integrating sustainable practices and circular economy principles in concrete industry. J. Environ. Manag. 370, 122702. https://doi.org/10.1016/j.jenvman.2024.122702.

Benoît, C., Norris, G.A., Valdivia, S., Ciroth, A., Moberg, A., Bos, U., Prakash, S., Ugaya, C., Beck, T., 2010. The guidelines for social life cycle assessment of products: just in time! Int. J. Life Cycle Assess. 15 (2), 156–163. https://doi.org/10.1007/s11367-009-0147-8.

Campo Gay, I., Hvam, L., Haug, A., Huang, G.Q., Larsson, R., 2024. A digital tool for life cycle assessment in construction projects. Dev. Built Environ. 20, 100535. https://doi.org/10.1016/j.dibe.2024.100535.

Chung, J.-H., Bae, B.-I., Choi, H.-K., Jung, H.-S., Choi, C.-S., 2018a. Evaluation of punching shear strength of voided slabs considering the effect of the ratio b_0/d. Eng. Struct. 164, 70–81. https://doi.org/10.1016/j.engstruct.2018.02.085.
Chung, J.-H., Jung, H.-S., Bae, B., Choi, C.-S., Choi, H.-K., 2018b. Two-way flexural behavior of donut-type voided slabs. Int. J. Concr. Struct. Mater. 12 (1), 26. https://doi.org/10.1186/s40069-018-0247-6.
Chung, J.-H., Jung, H.-S., Choi, H.-K., 2022. Flexural strength and stiffness of donut-type voided slab. Appl. Sci. 12 (12). https://doi.org/10.3390/app12125782.
Da Silva, T.R., de Azevedo, A.R.G., Cecchin, D., Marvila, M.T., Amran, M., Fediuk, R., Vatin, N., Karelina, M., Klyuev, S., Szelag, M., 2021. Application of plastic wastes in construction materials: a review using the concept of life-cycle assessment in the context of recent research for future perspectives. Materials 14 (13), 3549. https://doi.org/10.3390/ma14133549.
Ding, Z., Huang, X., Wang, X., Zuo, J., 2025. Assessment of promotional strategies for construction and demolition waste recycled products based on hybrid simulation system. Environ. Impact Assess. Rev. 112, 107814. https://doi.org/10.1016/j.eiar.2025.107814.
Dong, Y., Ng, S.T., Liu, P., 2023. Towards the principles of life cycle sustainability assessment: An integrative review for the construction and building industry. Sustain. Cities Soc. 95, 104604. https://doi.org/10.1016/j.scs.2023.104604.
Fanella, D.A., Mahamid, M., Mota, M., 2017. Flat plate–voided concrete slab systems: Design, serviceability, fire resistance, and construction. Pract. Period. Struct. Des. Constr. 22 (3), 4017004. https://doi.org/10.1061/(ASCE)SC.1943-5576.0000322.
Feiri, T., Kuhn, S., Wiens, U., Ricker, M., 2024. Designing for climate neutrality: evaluation of reinforced-concrete slab systems in regard to emission reduction targets. J. Build. Engineer. 95, 110220. https://doi.org/10.1016/j.jobe.2024.110220.
Feng, H., Zhao, J., Zhang, H., Zhu, S., Li, D., Thurairajah, N., 2022. Uncertainties in whole-building life cycle assessment: a systematic review. J. Build. Engineer. 50, 104191. https://doi.org/10.1016/j.jobe.2022.104191.
Ferdous, W., Manalo, A., Siddique, R., Aravinthan, T., Schubel, P., 2021. Recycling of landfill wastes (tyres, plastics and glass) in construction – a review on global waste generation, performance, application and future opportunities. Resour. Conserv. Recycl. 173, 105745. https://doi.org/10.1016/j.resconrec.2021.105745.
Gravina, R.J., Xie, T., Bennett, B., Visintin, P., 2021. HDPE and PET as aggregate replacement in concrete: life-cycle assessment, material development and a case study. J. Build. Engineer. 44, 103329. https://doi.org/10.1016/j.jobe.2021.103329.
Guaygua, B., Sánchez-Garrido, A., Yepes, V., 2024. Life cycle assessment of seismic resistant prefabricated modular buildings. Heliyon 10 (20), e39458. https://doi.org/10.1016/j.heliyon.2024.e39458.
Hafez, H., Bajić, P., Aidarov, S., Malija, X., Drewniok, M., Purnell, P., Tošić, N., 2024. Parametric study on the decarbonization potential of structural system and concrete mix design choices for mid-rise concrete buildings. Materials & Structures 57. https://doi.org/10.1617/s11527-024-02367-1. Article 85.
Haigh, R., 2025. A life cycle assessment of HDPE plastic milk bottle waste within concrete composites and their potential in residential building and construction applications. Urban Sci. *9* (4). https://doi.org/10.3390/urbansci9040116. Article 116.
Hernández, H., Ossio, F., Silva, M., 2023. Assessment of sustainability and efficiency metrics in modern methods of construction: a case study using a life cycle assessment approach. Sustainability 15 (7). https://doi.org/10.3390/su15076267.
Huijbregts, M.A.J., Steinmann, Z.J.N., Elshout, P.M.F., Stam, G., Verones, F., Vieira, M., Zijp, M., Hollander, A., Van Zelm, R., 2017. ReCiPe2016: a harmonised life cycle impact assessment method at midpoint and endpoint level. Int. J. Life Cycle Assess. 22, 138–147. https://doi.org/10.1007/s11367-016-1246-y.
Ingeli, R., Čekon, M., Paulovičová, L., 2025. Enhancement of the thermal performance of voided concrete slabs filled with expanded polystyrene. Case Stud. Construct. Mater. 22, e04567. https://doi.org/10.1016/j.cscm.2025.e04567.
Jiang, T., Yin, P., Jin, Q., 2024. Performances of typical photovoltaic module production from the perspective of life cycle sustainability assessment. Sust. Energy Technol. Assess. 64, 103703. https://doi.org/10.1016/j.seta.2024.103703.
Jin, R., Yan, L., Soboyejo, A.B.O., Huang, L., Kasal, B., 2018. Multivariate regression models in estimating the behavior of FRP tube encased recycled aggregate concrete. Constr. Build. Mater. 191, 216–227. https://doi.org/10.1016/j.conbuildmat.2018.10.012.
Josa, I., Borrion, A., 2025. Rebuilding or retrofitting? An assessment of social impacts using social life cycle assessment. Environ. Impact Assess. Rev. 112, 107794. https://doi.org/10.1016/j.eiar.2024.107794.
Lase, I.S., Ragaert, K., Dewulf, J., De Meester, S., 2021. Multivariate input–output and material flow analysis of current and future plastic recycling rates from waste electrical and electronic equipment: the case of small household appliances. Resour. Conserv. Recycl. 174, 105772. https://doi.org/10.1016/j.resconrec.2021.105772.
Li, L., Zuo, J., Duan, X., Wang, S., Chang, R., 2022. Converting waste plastics into construction applications: a business perspective. Environ. Impact Assess. Rev. 96, 106814. https://doi.org/10.1016/j.eiar.2022.106814.
Li, X., Xu, J., Su, Y., 2025. Research status and emerging trends in green building materials based on bibliometric network analysis. Buildings 15 (6). https://doi.org/10.3390/buildings15060884. Article 0884.
Lotz, M.T., Herbst, A., Müller, A., Kranzl, L., Rosales Carreon, J., Worrell, E., 2024. A material flow model of steel and concrete in EU buildings: national differences of the service-stock-flow nexus. Cleaner Waste Syst. 8. https://doi.org/10.1016/j.clwas.2024.100153. Article 100153.
MacArthur, E., Heading, H., 2019. How the Circular Economy Tackles Climate Change. Ellen MacArthur Foundation. https://content.ellenmacarthurfoundation.org/m/3eac8667edd240cc/original/Completing-the-picture-How-the-circular-economy-tackles-climate-change.pdf.
Metinal, Y.B., Gumusburun Ayalp, G., 2025. Uncovering barriers to circular construction: a global scientometric review and future research agenda. Sustainability 17 (4). https://doi.org/10.3390/su17041381.
Ministry of Transport, Mobility and Urban Agenda, 2021. Structural Code: Royal Decree 470/2021, of June 29. Government of Spain. https://www.boe.es/eli/es/rd/2021/06/29/470/dof/spa/pdf.
Navarro, I.J., Villalba, I., Yepes-Bellver, L., Alcalá, J., 2024. Social life cycle assessment of railway track substructure alternatives. J. Clean. Prod. 450, 142008. https://doi.org/10.1016/j.jclepro.2024.142008.
Nicácio, W.G., Barros, J.A.O., Melo, G.S.S.A., 2020. Punching behavior of BubbleDeck type reinforced concrete slabs. Struct. Concr. 21 (1), 262–277. https://doi.org/10.1002/suco.201900176.
Norouzi, M., Chàfer, M., Cabeza, L.F., Jiménez, L., Boer, D., 2021. Circular economy in the building and construction sector: a scientific evolution analysis. J. Build. Engineer. 44, 102704. https://doi.org/10.1016/j.jobe.2021.102704.
Paik, I., Na, S., 2019a. Comparison of carbon dioxide emissions of the ordinary reinforced concrete slab and the voided slab system during the construction phase: a case study of a residential building in South Korea. Sustainability 11 (13). https://doi.org/10.3390/su11133571.
Paik, I., Na, S., 2019b. Evaluation of carbon dioxide emissions amongst alternative slab systems during the construction phase in a building project. Appl. Sci. 9 (20). https://doi.org/10.3390/app9204333. Article 4333.
Paik, I., Na, S., Yoon, S., 2019. Assessment of CO2 emissions by replacing an ordinary reinforced concrete slab with the void slab system in a high-rise commercial residential complex building in South Korea. Sustainability 11 (1). https://doi.org/10.3390/su11010082.
Paranhos, R.S., Petter, C.O., 2013. Multivariate data analysis applied in hot-mix asphalt plants. Resour. Conserv. Recycl. 73, 1–10. https://doi.org/10.1016/j.resconrec.2013.01.009.
Patrisia, Y., Law, D.W., Gunasekara, C., Setunge, S., 2025. Assessment of waste-integrated concrete products: a cradle-to-cradle perspective. Int. J. Life Cycle Assess. 30, 834–861. https://doi.org/10.1007/s11367-025-02443-w.
Pavlů, T., Pešta, J., Vlach, T., Fořtová, K., 2023. Environmental impact of concrete slab made of recycled aggregate concrete based on limit states of load-bearing capacity and serviceability—LCA case study. Materials 16 (2), 616. https://doi.org/10.3390/ma16020616.
Pawar, A.J., Patil, Y.D., Vesmawala, G.R., Dhake, P.D., Nikam, J.S., 2024a. Two-way flexural behavior of biaxial voided slab using cuboidal shape of void formers. Structures 62, 106175. https://doi.org/10.1016/j.istruc.2024.106175.
Pawar, A.J., Patil, Y.D., Vesmawala, G.R., Dhake, P.D., Nikam, J.S., 2024b. Investigating the flexural behaviour of biaxial voided slab with varying size and spacing of cuboidal shaped void formers with innovative type of fixing reinforcement. Structures 64, 106616. https://doi.org/10.1016/j.istruc.2024.106616.
Penadés-Plà, V., Martínez-Muñoz, D., García-Segura, T., Navarro, I.J., Yepes, V., 2020. Environmental and social impact assessment of optimized post-tensioned concrete road bridges. Sustainability 12 (10). https://doi.org/10.3390/su12104265. Article 4265.
Poudel, S., Gyawali, T.R., 2025. Structural performance of symmetric and asymmetric plan irregular building structures: a comparative analysis of conventional and grid slab systems. Bull. Earthq. Eng. 23 (8), 3395–3420. https://doi.org/10.1007/s10518-025-02179-w.
Sagadevan, R., Rao, B.N., 2019. Effect of void former shapes on one-way flexural behaviour of biaxial hollow slabs. Int. J. Adv. Struct. Eng. 11 (3), 297–307. https://doi.org/10.1007/s40091-019-0231-7.
Salas, J., Yepes, V., 2018. Urban vulnerability assessment: advances from the strategic planning outlook. J. Clean. Prod. 179, 544–558. https://doi.org/10.1016/j.jclepro.2018.01.088.
Sánchez-Garrido, A.J., Navarro, I.J., Yepes, V., 2022. Multi-criteria decision-making applied to the sustainability of building structures based on modern methods of construction. J. Clean. Prod. 330, 129724. https://doi.org/10.1016/j.jclepro.2021.129724.
Sánchez-Garrido, A.J., Navarro, I.J., Yepes, V., 2024. Sustainable preventive maintenance of MMC-based concrete building structures in a harsh environment. J. Build. Engineer. 95, 110155. https://doi.org/10.1016/j.jobe.2024.110155.
Sánchez-Garrido, A.J., Navarro, I.J., Yepes, V., 2026. Optimizing reactive maintenance intervals for the sustainable rehabilitation of chloride-exposed coastal buildings with MMC-based concrete structure. Environ. Impact Assess. Rev. 116, 108110. https://doi.org/10.1016/j.eiar.2025.108110.
Scrucca, F., Ingrao, C., Barberio, G., Matarazzo, A., Lagioia, G., 2023. On the role of sustainable buildings in achieving the 2030 UN sustainable development goals. Environ. Impact Assess. Rev. 100, 107069. https://doi.org/10.1016/j.eiar.2023.107069.
Shanks, W., Dunant, C.F., Drewniok, M.P., Serrenho, A., Allwood, J.M., 2019. How much cement can we do without? Lessons from cement material flows in the UK. Resour. Conserv. Recycl. 141, 441–454. https://doi.org/10.1016/j.resconrec.2018.11.002.
Shen, L., Wang, L., Yang, Q., Ma, M., 2024. High-resolution mapping of urban residential building stock using multisource geographic data. Buildings 14 (5), 1266. https://doi.org/10.3390/buildings14051266.
Subramanian, K., Bhuvaneshwari, P., Jabez, N.A., 2017. Flexural behaviour of biaxial slabs voided with spherical HDPP void formers. Iran. J. Sci. Technol. Trans. Civ. Eng. 41 (4), 373–381. https://doi.org/10.1007/s40996-017-0077-9.
Traverso, M., Mankaa, R.N., 2025. The social life cycle assessment of products and organizations—methodological developments and implementations. Int. J. Life Cycle Assess. 30, 1011–1017. https://doi.org/10.1007/s11367-025-02480-5.

Tsui, T., Furlan, C., Wandl, A., Steger, S., 2024. Spatial parameters for circular construction hubs: location criteria for a circular built environment. Circ. Econ. Sustain. 4 (1), 317–338. https://doi.org/10.1007/s43615-023-00285-y.

United Nations Environment Programme (UNEP), Society of Environmental Toxicology and Chemistry (SETAC), 2009. Guidelines for Social Life Cycle Assessment of Products. https://www.lifecycleinitiative.org/wp-content/uploads/2012/12/2009%20-%20Guidelines%20for%20sLCA%20-%20EN.pdf.

United Nations Environment Programme (UNEP), Society of Environmental Toxicology and Chemistry (SETAC), 2013. Methodological Sheets for the Subcategories of Social Life Cycle Assessment (S-LCA). https://www.lifecycleinitiative.org/wp-content/uploads/2013/11/S-LCA_methodological_sheets_11.11.13.pdf.

Valivonis, J., Skuturna, T., Daugevičius, M., Šneideris, A., 2017. Punching shear strength of reinforced concrete slabs with plastic void formers. Constr. Build. Mater. 145, 518–527. https://doi.org/10.1016/j.conbuildmat.2017.04.057.

Visintin, P., Xie, T., Bennett, B., 2020. A large-scale life-cycle assessment of recycled aggregate concrete: the influence of functional unit, emissions allocation and carbon dioxide uptake. J. Clean. Prod. 248, 119243. https://doi.org/10.1016/j.jclepro.2019.119243.

Weidema, B.P., Wesnæs, M.S., 1996. Data quality management for life cycle inventories—an example of using data quality indicators. J. Clean. Prod. 4 (3–4), 167–174. https://doi.org/10.1016/S0959-6526(96)00043-1.

Yang, S., Long, R., Chen, H., Ma, W., Goh, M., 2025. How to promote sustainable recycling of plastic packaging waste? A study combining machine learning with gaming theory. Environ. Impact Assess. Rev. 112, 107819. https://doi.org/10.1016/j.eiar.2025.107819.